Tutora

Dra. Alicia Maestro Garriga
Departament de Ingenieria Química y Química Analítica

Secció de Ingenieria Química

Grau en Enginyeria Química

Treball Final de Grau

Study of the influence of Buchi encapsulator input variables on properties of formed alginate beads.

Estudio de la influencia de las variables de entrada del encapsulador Buchi en las propiedades de las esferas de alginato formadas.

Noemí Núñez Aguilar

June 2018

UNIVERSITAT DE BARCELONA

No temas a las dificultades,
lo mejor surge de ellas.

Rita Levi–Montalcin

En primer lugar, quiero agradecer a mi tutora la Doctora Alicia Maestro y a mi compañera de laboratorio Sharmaine Atencio, con las que he compartido muchas horas de trabajo y que me han ayudado y apoyado en todo momento.

También quiero dar las gracias a los doctores José María Gutiérrez, Carmen González y Esther Santamaría por sus recomendaciones y apoyo.

Y finalmente quiero dar las gracias a toda mi familia que me ha ayudado y apoyado en todo momento a lo largo de toda la carrera.

CONTENTS

SUMMARY

New techniques in food manufacturing have led the food industry to create foods with higher quality, organoleptic properties, better taste and new textures, and so-called functional foods, which include in their formulation some additives with especially healthy functions, delivering a high value product for customers and creating new markets. Innovation in the food industry is a key step to offer customers high quality products that meet their needs.

One of the ways to add and preserve the active ingredients to foods is their encapsulation in capsules of hydrogels. This work consists of studying the operation and production of the BUCHI Model-390 encapsulator by means of a composite central experimental design, in order to study the parameters that influence the production of capsules and their interactions and obtain a response surface to predict the Properties of the hydrogel spheres obtained fixed the input variables. Alginate was used as a hydrogel, and gelled by external gelation, dripping it with the BUCHI encapsulator over a calcium chloride solution. The properties of the alginate solution (molecular weight, viscosity, concentration ...) will influence the properties of the spheres.

The objective of the work is to control the shape and size of the sodium alginate spheres by modifying the operating variables of the Buchi encapsulator. In this study spheres without active ingredient will be prepared, but this work is intended to predict the behavior of spheres with encapsulated active ingredient. It must be taken into account that the viscosity of sodium alginate varies significantly with temperature.

By means of a factorial design it is observed that the input variables studied (frequency and position of the valve) have interaction with each other, and therefore their influence on the properties of the spheres can not be studied independently. For this reason, the composite central design is chosen to obtain the response surfaces.

The output variables to be studied are the output flow rate of the encapsulator, the average size of the spheres, the standard deviation of that size and the sphericity. Of the obtained, the

studied variables do not influence the sphericity and the standard deviation with a 95% probability in the studied range, but in the flow rate and the average size of the spheres. Response surfaces are obtained that are satisfactorily validated by experiments independent of the experimental design.

Keywords: Experimental design, encapsulator, sodium alginate, external gelation.

RESUMEN

Las nuevas técnicas en la fabricación de alimentos han llevado a la industria alimentaria a crear alimentos con propiedades organolépticas de mayor calidad, mejor sabor y nuevas texturas, y los llamados alimentos funcionales, que incluyen en su formulación algunos aditivos con funciones especialmente saludables, entregando un producto de alto valor para los clientes y creando nuevos mercados. La innovación en la industria alimentaria es un paso clave para ofrecer a los clientes productos de alta calidad que satisfagan sus necesidades.

Una de las maneras de agregar y preservar los principios activos a los alimentos es su encapsulación en perlas de hidrogeles. Este trabajo consiste en estudiar la operación y producción del encapsulador BUCHI Modelo-390 por medio de un diseño experimental central compuesto, con el fin de estudiar los parámetros que influyen en la producción de cápsulas y sus interacciones y obtener una superficie de respuesta para predecir las propiedades de las esferas de hidrogeles obtenidas fijadas las variables de entrada. Se usó alginato como hidrogel, y se gelificó mediante gelificación externa, goteándolo con el encapsulador BUCHI sobre una solución de cloruro de calcio. Las propiedades de la solución de alginato (peso molecular, viscosidad, concentración…) influirán en las propiedades de las esferas.

El objetivo del trabajo es poder controlar la forma y el tamaño de las esferas de alginato de sodio modificando las variables de operación del encapsulador Buchi. En este estudio se prepararán esferas sin principio activo, pero se pretende que este trabajo sirva predecir el comportamiento de esferas con principios activos encapsulados. Se debe tener en cuenta que la viscosidad del alginato de sodio varía significativamente con la temperatura.

Mediante un diseño factorial se observa que las variables de entrada estudiadas (frecuencia y posición de la válvula) tienen interacción entre sí, y por tanto su influencia en las propiedades de las esferas no puede estudiarse de manera independiente. Por ello se elige el diseño central compuesto para la obtención de las superficies de respuesta.

Las variables de salida a estudiar son el caudal de salida del encapsulador, el tamaño medio de las esferas, la desviación estándar de ese tamaño y la esfericidad. De los obtenidos se observa las variables estudiadas no influyen en la esfericidad y la desviación estándar con un 95% de probabilidad en el rango estudiado, pero sí en el caudal y el tamaño medio de las esferas. Se obtienen superficies de respuesta que son validadas satisfactoriamente mediante experimentos independientes al diseño experimental.

Palabras clave: Diseño experimental, encapsulador, alginato de sodio, gelificación externa.

1. INTRODUCTION

In the last decades, functional foods have been used more and more frequently, which are elaborated not only for their nutritional characteristics but also to fulfil a specific function such as improving health and reducing the risk of contracting diseases (Lopez-Rubio, Gavara, & Lagar_on, 2006). One of the most used techniques to protect these foods is the microencapsulation technique with sodium alginate. Alginate has been one of the most used polymers thanks to its highly versatile, biocompatible and non-toxic matrix for the protection of active components, cells or microorganisms sensitive to heat, pH, oxygen and light, among other factors, to which they are exposed. the food during processing and storage (Funami et al., 2009). The process of microencapsulation with alginate is carried out through two mechanisms of ionic gelation: external gelation and internal gelation, depending on whether calcium is supplied from outside the capsules or inside them.

1.1. MICROENCAPSULATION AND ITS APPLICATIONS

Antioxidants like vitamins, phenol, flavonoids and proanthocyanidins retard or inhibit oxidation of lipids and prevent certain diseases (Kris-Etherton et al., 2004; Owen et al., 2000; Woodside et al., 1999), such as cancer, artherosclerosis, neurodegenerative, inflammatory and cardiovascular diseases (Prior & Gu, 2005). Flavonoids polyphenolic compounds are widely distributed among plants mainly in seeds, fruits and beverages such as tea, wine and beer. The antioxidant activity of the phenolic compounds is mainly due to their redox properties, as they play an important role by neutralizing free radicals and oxidants (Feng Peng et al., 2003). Considering the above benefits and new ideas to reduce the use of commercial synthetic antioxidants, natural extracts rich in polyphenols arise as active ingredients that may be incorporated into food in order to make it functional.

Because the addition of natural antioxidants may alter the color and flavor of foods, recent studies suggest the application of microencapsulation technique to mask these effects, to protect them from the environment or for controlling release into food (Champagne & Fustier, 2007; Deladino, Anbinder, Navarro, & Martino, 2008).

One of the most used techniques to protect and mask substances is the microencapsulation technology with sodium alginate (ME). The microencapsulation (ME) technique has been mainly described as a process in which small particles or droplets are surrounded by a homogeneous or heterogeneous coating, forming beads or capsules with various applications (Borgogna, Bellich, Zorzin, Lapsin & Cesáro, 2010). In this sense, microparticles, microcapsules or microspheres are defined as the product of the microencapsulation process depending on their morphology and internal structure (Anal & Singh, 2007). The process of microencapsulation with alginate is carried out through two mechanisms of ionic gelation: external gelation and internal gelation, depending on whether calcium is supplied from outside the capsules or inside them.

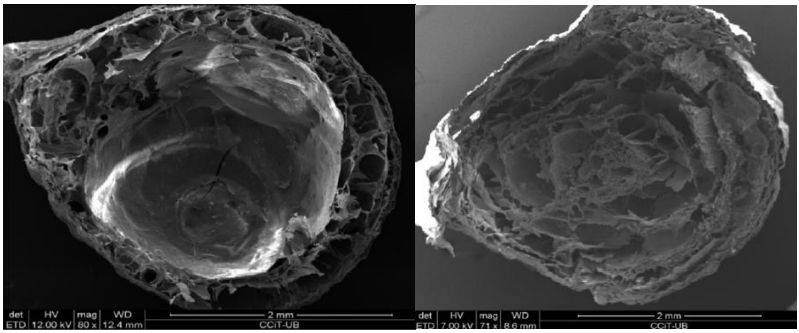

a) b)

Figure 1. SEM Microphotographs of lyophilized beads at 1.10^3 mol Ca^{+2}/g alginate (high calcium concentration) a) External microencapsulation b) Internal microencapsulation (From Lupo et al., 2015)

The external gelation process occurs with the diffusion of the calcium ion from a source surrounding the hydrocolloid to the alginate solution. The formation of the gel starts at the interface and progresses inward as the surface is saturated with calcium ions, so that the sodium ion from the alginate salt is displaced by the divalent cation solubilized in water. Although the most used calcium source is $CaCl_2$ due to its higher percentage of available calcium, there are other less

frequently used salts such as acetate monohydrate and calcium lactate (Helgerud et al., 2010). In Figure 1 a) it is observed how the outer layer has gelled, leaving inside the microcapsule the encapsulated product that in this case has not gelled, but can do so.

The internal gelation process consists of the controlled release of calcium ion from an internal source of insoluble or partially soluble calcium salt dispersed in the sodium alginate solution. Where the release of calcium ion can occur in two ways, if you have an insoluble calcium salt at a neutral pH but soluble at acidic pH, it is necessary to add an organic acid that, when diffused to the salt, allows the acidification of the medium and solubilize calcium ions. As seen in Figure 1 b), the gelation occurs in the whole drops, so, more homogeneously, meaning a more regular form of the microcapsule.

1.2. SODIUM ALGINATE AND ITS USE FOR THE MICROENCAPSULATION

Sodium alginate is a natural polysaccharide extracted from several species of brown seaweed. It is composed of linear copolymers arranged in blocks composed of residues of (1 → 4) - β-D-mannuronate (M) and α-L-guluronate (G) (Draget & Taylor, 2011). Among its most important properties lies the ability to prepare gel structures when the carboxyl group, belonging to the G blocks, produces crosslinking when it meets double valence cations.

Alginate is one of the most widely used polymers in microencapsulation, as it forms a highly versatile, biocompatible and nontoxic matrix of gel that can protect active components of factors such as heat, pH, oxidation and moisture action thereby enhancing stability and bioavailability (Funami et al., 2009). Moreover, alginate has many advantages both for human consumption and industrial application. Such aspects are compiled in the literature by Imeson (2010, Chap. 4), highlighting the prebiotic effect of the low molecular weight alginates, their benefits as daily fiber intake for the reduction of cholesterol levels in blood sugar and their ability to extend product shelf life (Goh, Heng, & Chan, 2012).

The process of gelling occurs in the presence of multivalent cations (except magnesium) where the calcium ion is the most used by the food industry. The gelation takes place by producing a binding zone between a G-block of a cotton molecule that is physically linked to another G-block contained in another cotton molecule through calcium. The visualization of the physical structure is called the "egg box" model by Draget (2000), shown in Figure 2 (Reddy-K and Reddy, P., 2010).

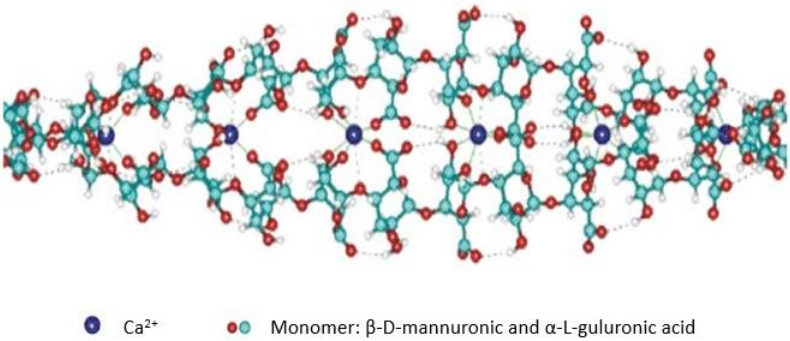

Figure 2. Model "egg box" (From Lupo et al., 2014)

Among the most used salts of alginate, the sodium salt has been found due to its high solubility in cold water and characteristic sol-gel transition instantaneously and irreversibly to the calcium ion (Funami et al., 2009).

The selection of the appropriate encapsulation technique is determined by the physical-chemical properties of the support material and the final application desired to ensure the bioavailability of the compounds, their functionality and even their easy incorporation into the food without the alteration of the its sensory properties (Pal et al., 2009). By using alginate as a polymer matrix, microencapsulation techniques in food applications are reduced to: extrusion, emulsion and spray drying.

This work will focus on the extrusion technique which consists in forming droplets of the alginate solution containing the component to be encapsulated by passing said solution through an extruder device of controlled drip size and speed. These drops fall on a bath containing the source of the divalent ion, which induces gelation through the mechanism of external gelation (Chan et al., 2009). The size and shape of the capsules formed depend mainly on the nozzle of the extruder device, which can be manual (syringe, pipette ...) or automatic, as is the case of the Buchi encapsulator, recently acquired by the research group with which the study will be carried out. Another factor that will significantly affect the size and shape of the capsules is the flow rate, which will depend on the viscosity of the sodium alginate solution. Also noteworthy is the

separation distance from the nozzle to the bath, the effect of gravity and the surface tension of the solution that induces gelation (Chan et al., 2009).

1.3. BUCHI ENCAPSULATOR MODEL B-390

The Buchi encapsulator offers sophisticated encapsulation technology to produce uniform beads and capsules at a high reproducibility rate. It consists of a system that allows to fix the overpressure through a wheel, which together with the outlet valve regulates the flow of alginate solution depending on its viscosity and the nozzle chosen. It has a system of nozzles with different sizes which will mainly affect the diameter of beads. It is also provided of a vibratory unit that works with a frequency that can be varied in order to cut the outlet flux into droplets that will fall on the calcium bath. It also has a plug for grounding wire, a magnetic field to separate the capsules at the exit and a stroboscope lamp to see more easily the chain of capsules that is formed.

1.4. VARIABLES INVOLVED IN THE PRODUCTION OF ALGINATE CAPSULES

To develop a good experimental design, it is important to highlight the parameters that influence the encapsulation. The parameters described below are directly involved in the operation of the Buchi encapsulator.

1.4.1. Concentration of Alginate Solution

To produce spherical alginate beads, the optimum concentration for an alginate solution prepared from low-molecular-weight alginate with intrinsic viscosity of 954mLg–1 is around 8% w/v, while for the high-molecular-weight alginate (e.g., 519500), spherical beads could be produced with a concentration around 1-2% w/v alginate solution (Fundueanu et al., 1999). Lower concentrations produce a too weak gel matrix and higher ones present a viscosity of alginate before gelation too high to be managed and a marked syneresis (they exude water) (Milián, 2017). Mahajan et al. (2010) reported that alginate beads (at concentrations 1,1.5 and 2%) were spherical in shape and at lower concentrations (below 1%) their shape was not perfectly spherical

and were mainly elliptical, ovoid in shape (Mahajan, Gupta, & and Sharma, 2010). Moreover, Garcia et al. (2017), who encapsulated Cyanex 302 with alginate for palladium recovery, demonstrated that the best alginate beads (without extractant) can be obtained using high-viscosity alginate (i.e. high molecular weight alginate) at the concentration of 1% (w/w).

1.4.2. Concentration of calcium chloride

It has been reported that it is impossible to produce beads at Ca^{2+} concentrations below 0.005M and 0.01M for the low M / G ratio alginate and the high M / G ratio alginate, respectively. As a rule of thumb, the typical concentration of calcium chloride prepared for alginate bead formation is 0.1M (Lee, Ravindra, & Chan, 2013), which is equal to 1.1098% w / v by stoichiometry. Lupo-Pasin (2015) analyzed the M / G ratio of the sodium alginate procured from Panreac by Nuclear Magnetic Resonance (NMR) and reported a ratio value of 1.43. Results showed that the sample was composed of 58.85% M and 41.15% G. For this, a concentration of 1% w / v for the calcium chloride is used in this study.

1.4.3. Pressure

Based on the pre-determined parameters of the Buchi Encapsulator 390 used to produce alginate beads in the size range of 1150-1800 µm for the 750 µm nozzle size, the recommended range of air pressure for the selected nozzle is 300 to 500 mbar (Whelehan, 2014).

1.4.4. Nozzle size

Prüsse et al. (2008) noted that the vibrating nozzle technique, which is the principle employed in the Buchi Encapsulator B-390, is capable of producing alginate microgels with a large size range of 300 µm to 5 mm (Prüsse et al., 2008). In the single nozzle configuration, the bead diameter is approximately twice the nozzle diameter size (Whelehan, 2014). Anyway, the nozzle size has to be in accordance to the viscosity of alginate solution that has to go through. Roughly, a solution with high viscosity will require a nozzle with higher diameter than one with a lower viscosity, as otherwise the pressure drop across the nozzle would be too high and the flow could be prevented.

1.4.5. Electrode

During formation of the droplet chain, there is a necessity to disperse newly created spheres to prevent agglomeration and coalescence which are unwanted in the process because these will lead to agglomerates of double or triple volume. In the Buchi Encapsulator B-390, the dispersion of the spheres is accomplished by electrostatic repulsion forces system which charges the droplets right after breakup in order to eliminate agglomeration effect. Bradenberger et al. (1999) presented a method to prevent coalescence by charging the droplets with a high voltage electrode in the range of 400 to 1400 V to produce polymer beads of 160 to 800 μm in diameter (Brandenberger, Nussli, & Widmer, 1999). However, Whelehan (2014) reported in the laboratory guide for the use of the Buchi Encapsulator B-390 that the electrode voltage has no influence on bead size and encapsulation productivity, as long as it is enough to avoid agglomeration.

1.4.6. Amplitude of vibration

Amplitude refers to the intensity of the vibration. As the amplitude increases, the vibration becomes stronger. The amplitude of the encapsulator can be set from 1 to 9. Based on the equipment manual of the encapsulator, the amplitude setting of the vibration has minimal influence on the bead size and encapsulation productivity (Whelehan, 2014). However, too high value of the amplitude can cause an unstable liquid stream (BUCHI Labortechnik AG, 2016).

1.4.7. Valve position

The position of the valve affects the output flow, because a closed valve provides a loss of load to the circulating fluid. The valve is regulated manually, so that the more closed it is, the narrower the conduit through which the fluid flows, preventing the passage of this, generating a greater loss of load, for which it will foreseeably affect the size, shape and productivity of the formed spheres. The higher the flow, the greater the opening of the valve, the larger spheres are expected (Whelehan, 2014).

1.4.8. Frequency

The frequency is defined as the vibration that is breaking the flow rate applied in the unit producing beads, affecting in the size of drop, depending on whether the frequency is more or less high. A high frequency generates a higher production but a smaller drop size, and as the frequency decreases, the drop size increases, since the flow of fluid is greater than each break due to vibration. The frequency of the encapsulator can be set from 80 to 2000 (Whelehan, 2014).

Due to the influence of these factors, it is expected that when varying the properties of the capsules will vary significantly, so it is interesting to study how they affect the factors (frequency and position of the valve) in the spheres obtained by the Buchi encapsulator.

2. OBJECTIVES

The main objective of this work is to quantify the influence of the independent variables that must be fixed in the BUCHI encapsulator and that, according to the manual, are the most relevant, in the properties of the beads formed. A high molecular weight alginate at a concentration of 1% is used as the hydrocolloid, gellified by dropping over a calcium solution. Outer variables studied were mean bead diameter, standard deviation of diameter, flow rate of the encapsulator and sphericity.

To carry out this main objective, these sub goals will be carried out:

1. Study of the range of work.
2. Study of the appropriate experimental procedure by:
   - Comparison of the results obtained by two experimenters in order to determine if results are affected by who carries out experiments.
   - Size of the population to obtain reproducible results in order to fix the minimum beads that must be measured.
3. Through a factorial design at two levels, study whether there are interactions between the 2 input variables to be studied, valve opening a frequency.
4. Analyze which factors affect the different responses studied in a statistically significant, through a central composite design and Pareto analysis.
5. Obtain a response surface that allows estimating the different response variables by knowing the input variables through a central composite design (CCD).

Validate the model obtained through independent experiments that corroborate that the model can predict the response with 95% probability.

3. MATERIALS AND METHODS

In this chapter, it is described the experimental methodology that has been used to carry out this work. In the first place, the corresponding substances and materials used in the work are listed. Next, the experimental device for encapsulating and preparing the different solutions used is described. Finally, the base of the experimental design is briefly developed. This experimental strategy has allowed us to plan and program the necessary research to study and optimize the bead formation process.

3.1 MATERIALS

The solutions prepared in this work are constituted by different substances that are described below in more detail.

3.1.1. Components for solutions

Milli-Q water

Calcium chloride anhydrous, granular, ≤7.0 mm, ≥93.0% (Sigma-Aldrich) MW=110.98 g/mol

Sodium Alginate LS (Panreac)

3.1.2. Equipment

Magnetic Stirrer RCT basic IKA 0-2500 rpm in order to prepare solutions and provide agitation of the $CaCl_2$ solution during dropping of alginate solution from the Buchi encapsulator.

OPTIKA Vision Pro (OPTIKA Microscopes, Italy) mounted with OPTIKAM Pro 5LTO in order to obtain pictures of beads

BÜCHI Encapsulator Model B-390

Ultra-Turrax model T25 basic IKA WERKE in order to prepare solutions of sodium alginate 1%.

Analytical balance Kern model ABJ-NM/ ABS-N, capacity 200 g and precision of 0.1 mg

Flask of different sizes

Beakers of different sizes

3.1.2.1. Optika microscopy Italy

The Optika microscope is composed of a camera integrated in the head and different magnifications. Through a proper software images and videos are transferred in real time to a computer for further processing of data. Its resolution is of high quality, so the length of the measurements is as accurate as possible. Optika does not import calibrated, so in each use it must be calibrated to have a measure in accordance with reality. For this a metric scale is used that comes with the microscope.

Its advanced software can do all kind of data processing, of which it is worth highlighting, the measurement, the counting and the export to excel of said data.

3.2 METHODOLOGY

3.2.1 Preparation of stock alginate solution

The sodium alginate solution is prepared by weighing sodium alginate powder on an analytical balance according to the desired concentration. The powder is transferred to a beaker and then the respective deionized water is added to prepare solutions at the desired percentage (1%, according to Fundueanu et al., 1999). The solution is homogenized using an Ultra-Turrax stirrer, which uses a high shear, at room temperature. Once the solution is completely homogenized, it is stored for 24 hours inside the refrigerator to allow it to hydrate and eliminate all the air bubbles it contains because of the agitation. All polymer solutions were prepared 24 hours before their use in the encapsulator.

3.2.2 Preparation of stock calcium chloride

The calcium chloride solution is prepared by weighing this calcium salt granules on an analytical balance according to the desired concentration. The weighted mass is transferred to a beaker and then the required deionized water is added to prepare the desired solution (1%, according to Lupo-Pasin (2015)). The solution is mixed using a magnetic stirrer, at a high speed

at room temperature. Once the solution is completely homogenized, let it stand for 5 minutes and use it for the necessary experiments. Said solution is not necessary to cool as it happens in the sodium alginate since no air bubbles are produced inside.

3.2.3 Production of Alginate Beads using the BÜCHI-390 Encapsulator

The 750-µm diameter single nozzle was attached to the assembled bead producing unit of the encapsulator. The vibration unit was then placed on the bead producing unit. A beaker containing 100-mL of 1% w/v calcium chloride solution was placed below the nozzle and a magnetic stirrer was added in the beaker so that a slight vortex was visible. The grounded clip was placed over the edge of the beaker and into the liquid.

The feeding bottle was firstly filled with the alginate solution and screwed on the assembled cap. The silicon tube was passed between the blades of the liquid flow regulating valve and the male luer lock fitting of the silicon tube was attached to the female luer lock fitting of the bead producing unit. The valve was squeezed by turning the knob clock wise so that the silicon tube is closed. The external pressurized air supply was opened in order to pressurize the feeding bottle, and the value was set to 400 mbar overpressure. The electrode and the amplitude were set at 350 V and 6, respectively.

The vibration control system was activated, and the vibration frequency was set at the desired level based on the design of the experiment which is discussed in the next section. The liquid flow regulating valve was opened by turning the knob counter-clock wise until the liquid flows through the silicone tubing and the bead producing unit to the nozzle where it forms a continuous liquid jet. The opening of the valve was regulated based on the assigned values as detailed in the design of the experiment. The visible bead chain is monitored through the light of the stroboscope lamp.

3.2.4 Measurement of Flow Rate of Alginate Solution During Encapsulation

Prior to the experiments, the density of the prepared 1% (w/v) alginate solution was measured. Alginate density was obtained using a graduated flask of known volume, previously tared. With the weight difference of the graduated divided volume flask the sodium alginate dye

was obtained experimentally. The alginate solution feed line was connected to the Encapsulator B-390. The independent parameters (amplitude, electrode tension and air pressure, as discussed previously) of the encapsulator were set and activated. The flow rate was measured for each experimental condition (for a given combination of frequency and valve opening position values based on the experimental design).

The beaker placed below the nozzle was covered first with a plate (Petri dish). After setting all the independent parameters of the encapsulator, the desired frequency (for first run of experiment) was activated. Then, the liquid flow regulating valve was opened by turning the knob counter clock wise to its desired first value (based on the experimental design) until the solution flows through the silicone tubing and the bead producing unit to the nozzle where it forms obtain a good drop chain in the light of the stroboscope lamp. As soon as a symmetrical and stable dispersal was obtained, a small empty beaker (previously weighed) was placed directly below the nozzle to collect the alginate beads being formed. The flow of the alginate beads was collected for exactly 30 seconds. After this, procedure it was started with the corresponding experiment.

Flow rate will be calculated as follows:

$$flow\ rate\ \left(\frac{ml}{s}\right) = \frac{\frac{(\text{weight of alginate solution collected in the beaker in grams})}{\text{density of alginate solution in g/ml}}}{30\ \text{seconds}} \quad \text{[Eq.1]}$$

3.3 EXPERIMENTAL DESIGN

Next, the theoretical basis of the experimental design that has been used to plan the experimentation of this work is described. Likewise, the methods of analysis and interpretation of results are described.

3.3.1 Factorial design

The factorial design is used in experiments that include several factors when it is necessary to study the joint effect of the factors on a response. This design allows to explore a chosen area of the experimental domain and find a promising direction for the subsequent optimization.

It is called factors to all those input or independent variables that may affect the process and, therefore, response, output or dependent variables. There are considered output response or variable response to the different properties of the obtained samples (flow rate, bead diameter, standard deviation of diameter distribution and sphericity).

3.3.2 Factorial design at two levels

A factorial design is used at two levels because it allows roughly to calculate the effect of each input variable on a response variable, as well as the possible interactions between the different input variables. It means that the effect of one variable may not be the same at different levels of the other one. If this is the case, effect of each variable cannot be studied separately and an experimental design where variables are simultaneously changed is required. Factorial design allows to identify the critical process variables and to determine which direction the following experiments should follow.

For a factorial design at two levels, a lower and upper level of each input variable must be chosen. The number of experiments to be performed would therefore be 2^k where k corresponds to the total number of input variables studied. Figure 3 shows the experimental domain and the programmed tests for a factorial design at two levels of two variables.

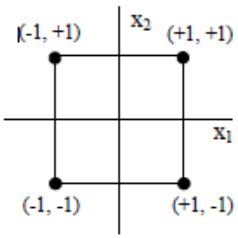

Figure 3. Experiments of a factorial design composed of two variables at two levels.

From the responses determined for each of the programmed experiments, the main effect of a variable on the output response [Eq.2] is defined as the change experienced by the response with the change of a variable from its lower level to the higher one, for all possible combinations of the rest of the variables. Therefore, it corresponds to the difference between the means of the responses obtained from the experiments carried out in the upper level of the variable minus the responses obtained in the lower level.

Main Effect= $y^+ - y^-$ [Eq.2]

Interaction is defined as the influence that a change in an input variable can have on the effect of another input variable on the output response. You can analyse the interaction of two variables representing the response as a function of a variable, x_1, for the two levels studied of another variable, x_2. When the difference in response between the two studied levels of a variable, x_1, is not the same at all levels of another variable, x_2, it is considered that interaction exists [Fig. 4]. It can be observed that lines are not parallel. When this occurs, one variable should not be studied independently of the other, since the effect of one variable will depend on the value of the other variable.

On the contrary, if the difference of response for each level of x_1 at different levels of x_2 is the same, that is, if the lines are parallel [Fig. 4], it is considered that there is no interaction between x_1 and x_2. In this case, each variable could be studied independently.

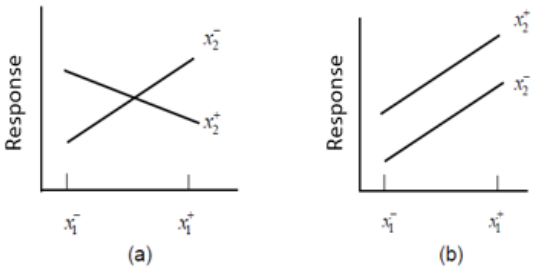

Figure 4 (a) Interaction between variables x_1 and x_2 (b) No interaction between variables x_1 and x_2

3.3.3 Central composite design (CCD)

For a more accurate study of the effect of input variables (factors) on the response ones, especially when interactions occur, a type of experimental design used is the central composite design (CCD). This design allows to describe non-linear behaviours, since each factor is studied at three or more levels. The CCD is the most popular class of designs used for fitting second-order models. Generally, the CCD consists of a 2^k factorial design (two-level factorial design, k=number of input variables), 2^k axial or star runs, and n_c centre runs. Figure XX shows the CCD for k=2 factors. There are two parameters in the design that must be specified: the distance α of the axial runs form the design centre and the number of centre points, n_c.

It is recommended for a second-order response surface design to be rotatable. This means that the variance and, therefore, the accuracy in prediction, is the same at all points that are at the same distance from the design centre. A CCD is made routable by the choice of α according to Eq. XX, where N_c is the number of experiments of the factorial design. For k=2, $\propto = \sqrt{2}$, the star points corresponding to a rotation of the factorial design points, all at the same distance from the center. The number of center runs is usually between 3 and 5 (Montgomery, 2001).

For the example in Figure 5, k=2, and 3 runs of central point, 11 experiments are required.

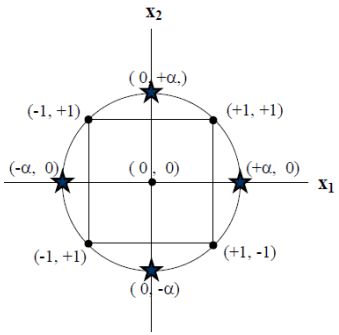

Figure 5. Central composite design for two

3.3.4 Analysis of the design of experiments

Once the experimental data are collected, the next stage of all experimental research consists in the analysis and interpretation of the results obtained. The factorial designs plan the experiments in such a way that they can be analysed by statistical methods giving satisfactory results. The most usual way to express the results is to adjust by regression the experimental data obtained to empirical models that relate the response variable according to the variables studied.

The rotatability in the composite central design only depends on the value of α and the number of experiments corresponding to the complete factorial design that is part of the composite central design [Eq. 3]. Thus, for a central design composed of two variables, the value of α corresponds to √2.

$$\alpha = \sqrt[4]{N_c} \qquad \text{[Eq.3]}$$

The number of replicas that must be made in the central point of the composite central design are 3 for a good fit of the design.

The objective is to obtain parameters (b_0, b_1, ..., b_n) that minimize the sum of squares $\sum(yi - \bar{y})^2$, where y_i are the experimental values and $\hat{y}$ represents the estimated value. In Equation XX, an example of a second-degree polynomial experimental model is shown for two variables. As mentioned above, the coefficients, b_i, as well as the error term, ε, are estimated by regression from the experimental data.

$$y = b_0 + b_1 \cdot x_1 + b_2 \cdot x_2 + b_3 \cdot x_1^2 + b_4 \cdot x_2^2 + b_5 \cdot x_1 \cdot x_2 + \varepsilon \qquad \text{[Eq.4]}$$

Once the empirical model is obtained by regression, an analysis must be made to determine which parameters are significantly important and which are due to experimental error. One of the most used methods is the Analysis of Variance, a statistical tool that allows analysing and comparing the variances of different data series. In the context of the design of experiments, this analysis compares and evaluates the variance of the response variable for the two populations studied: the experimental data and the values estimated by the model.

For the application of the analysis to be correct, three requirements must be met: data corresponding to each population should be simple random samples of their corresponding populations, the populations from which each sample comes should be normal and of the same variance (Prat et al., 1997). In the case of the third requirement, the residual graphs (observed value less mean of the sample) versus estimated values are very useful. Figure 6 shows a Residues Chart showing how residues are distributed randomly. In this case, it can be concluded that there is no indication that the variability (variance) is different between the two populations studied, assuming the third requirement for the application of an Analysis of Variance between two populations.

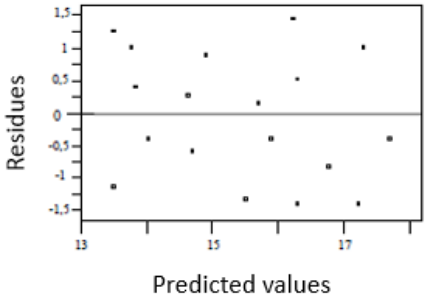

Figure 6. Example of a Residual graph.

The Pareto Chart of the standardized effect (Figure 7) indicates that the effects of the two experimental variables and their interaction are statistically significant. The Pareto Chart displays the absolute value of the effects and draws a reference line on the chart at t-value limit, where t is the (1 - α / 2) quantile of a t-distribution with degrees of freedom equal to the degrees of freedom for the error term Statistically insignificant (Kukreja et al., 2011). These diagrams are adjusted to a level of probability, normally 95%, in which the variables that exceed the line influence significantly, while those that do not exceed the line do not affect and therefore are not necessary to consider. Using the Pareto diagram, the equations that define the central composite design (CCD) are developed.

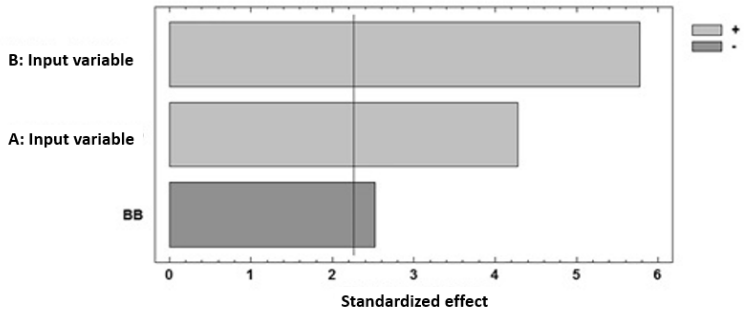

Figure 7. Example of a Pareto diagram.

The analysis of variance is used to compare if the values of a set of numerical data are like the values of another or more data sets. The method to compare these values is based on the global variance observed in the groups of numerical data to be compared.

The ANOVA starts from some assumptions that have met:

- The populations (probability distributions of the dependent variable corresponding to each factor) are normal.
- The K samples on which the treatments are applied are independent.
- The populations all have the same variance.

The Analysis of Variance is based on the construction and analysis of a table called "ANOVA table" (ANalysis Of VAriance) which shows the sum of squares, the degrees of freedom and the average squares provided by the statistical program. These allow to calculate statistics as the distribution function F, probabilities that a change in the response is due to the experimental error at different levels of significance, confidence intervals, the regression coefficient (R^2), the corrected regression coefficient ($R^2_{corr.}$).

The regression coefficient is always between 0 and 1. In this case, it is considered that the model describes in the percentage of the regression coefficient obtained the variability of the response as a function of the variables studied. The regression coefficient must be the closest to one for the adjustment to be considered good. The corrected regression coefficient ($R^2_{corr.}$) is

more suitable for validating models with several independent variables, since it considers the degrees of freedom of the system.

4. RESULTS AND DISCUSSION

In this chapter it will be studied the influence of the factors frequency and valve opening of the Buchy equipment in the resulting flow rate and the diameter, standard deviation and sphericity of obtained beads. As we were two people working in the same laboratory and the same equipment, first of all it must to be stablished if we two worked in the same way, or statistically different results were obtained if I or my partner developed the same experiment. It was done regarding to flow rate and bead size measurements.

Once stablished, it must to be determined the size of population (number of beads to be counted) in order to obtain proper results.

After that, range of work for factors (variables) and the other fixed variables are chosen. Then, a factorial design at two levels is developed in order to roughly determine which factors affect to response variables and if interactions occur. Finally, a CCD is carried out in order to obtain a surface response for a quadratic fitting to be able to predict response variables.

A validation of the model is further required through the use of new independent experiments, in order to prove if the model is valid.

4.1 COMPARE POPULATIONS

To guarantee reliable and statistically significant results regardless of who or how the process is developed while maintaining the established parameters, statistical studies are carried out for each case.

4.1.1 Comparison of flow rate measurements

The first task was to compare whether at the time of entering the parameters in the Buchi encapsulator my partner and I were significantly different or not. For this we made different

collected volume measurements (10 for person) for a time (10 seconds) to calculate flow, each time placing the valve opening at the set point starting from zero.

By means of a difference in weight and the calculation of the density of the alginate solution used, the flow rate values are obtained. With these values and through the Statgraphic Centurion XVII program, the population study is performed by the ANOVA method. When comparing the populations, it is obtained that there is no significance with a confidence level of 95%, so that it is independent who regulates the valve for obtaining the flow rate.

4.1.2 Comparation of populations for size measurement

Other important aspect to consider was if my partner and I measured the size of capsules in the same way, and therefore, whether it influenced who determined the capsule size. For this, she and I measured the same population of spheres (the same pictures) and then we checked whether the values obtained by each one of us were significantly different or not. For this the Statgraphics Centurion XVII program was used.

To obtain a good precision in the determination of the results, the population was measured three times for each one of us on different days. The results were the following.

Table 1. Mean values of diameters.

		Mean lognormal
Sharmaine	1	1321,78
	2	1323,98
	3	1305,18
Noemí (I am)	1	1206,06
	2	1222,36
	3	1206,06

Previously to the analysis by means of the ANOVA method it can be observed that measurements of Sharmaine and me for the same population are clearly different, since the measurements of my partner are in the order of 1200 and mine in the 1300.

Anyway, the analysis of variance through the Statgraphics Centurion XVII program was carried out. It was obtained that for the mean values the confidence interval did not contain the the value

0 and therefore there was a statistically significant difference between the means of the two samples, with a confidence level of 95%. Therefore, from now on only one of us will measure beads to remove the effect of who measure them.

4.1.3 Comparison of populations: size population

At the time of carrying out the work, it was important to know how many capsules were necessary to count in order to obtain statistically significant results, i.e. the size of sample. For this, the study of two populations of 100 capsules obtained for two runs of experiment with the same conditions (frequency and valve position) was carried out. When doing the analysis of variance ANOVA with a confidence level of 95% it was found that they were significantly different, so the size of 100 was too small.

Next, two new populations were studied, this time with 400 capsules each. The two experiments had the same conditions as for the populations of 100 capsules. The results were analyzed by means of ANOVA with a confidence level of 95% and it was determined that they were statistically the same, so that a population of 400 capsules was enough to guarantee a reliable experimental design.

4.2 ESTABLISHING THE RANGE

A modified intuitive approach, Changing One Separate factor a Time (COST) (Mazzitelli et al., 2008; Tosi, Balestra, & Nastruzzi, 2008), was employed to define the crucial ranges of vibration frequency and position of the valve (valve opening) that are feasible for alginate bead production. In this approach, bead production was carried out by keeping six parameters at a constant value (air pressure, electrode voltage, amplitude of vibration, nozzle diameter, and concentrations of the alginate solution and calcium chloride bath) in all the experimental runs, while frequency and valve opening were being investigated.

4.2.1. Selection of the Constant Parameters for the Microencapsulation Process

The following paragraphs discusses the bases for defining the values used for the constant parameters.

- Concentration of Alginate Solution (1% w/w)

In this experimental design, the concentration of alginate solution to produce alginate beads is kept constant at 1% w/v because it has a high molecular weight. Alginate composition, sequential structure and molecular weight (*Mw* and *Mn*) was determined in a previous study conducted by Lupo-Pasin (2015), who reported that the average molecular weight of the same alginate samples used is 1750 kDa while the average numerical molecular weight (*Mn*) is 668 kDa. As explained in the introduction section 1.4, the lower values produce a too weak gel matrix and the high frequencies have an alginate viscosity before gelation too high to be handled.

- Concentration of Calcium Chloride Solution (1%)

As discussed in the introduction (section 1.4, Lupo-Pasin (2015)), the proper calcium chloride concentration is 1%. This concentration guarantees a complete gelation since the calcium ions are sufficient to penetrate the entire surface of the calcium alginate forming stable capsules and avoids syneresis.

- Overpressure (400 mbar)

An experimental study based on the predetermined range by Buchi encapsulator was made, and it was determined that the optimum overpressure for a good working range was 400 mbar. For higher and lower overpressures, the range of work in which acceptable capsules were obtained was zero (Milián, 2017).

- Nozzle size (750 µm)

In this experimental design, the nozzle size diameter used was 750 µm, to produce alginate beads in the size range of 1150 – 1800 µm (Whelehan, 2014). With this size of nozzle, we can guarantee an adequate size of capsules, large enough without exceeding that they will allow a good study of the different responses. As explained in the introduction (section 1.4) for the selected alginate concentration (1%) this is the optimal size of nozle.

- Electrode (350V)

To avoid the agglomeration of the capsules at the outlet of the encapsulator, an electromagnetic field is necessary, but as described in the introduction, said field does not affect the production of capsules, with a minimum value to prevent agglomeration. Tests have been made for the verification of this theory for the Buchi encapsulator and the theory is reaffirmed, for which the value of 350V (default value) has been set.

- Amplitude of Vibration (6)

The amplitude of vibration does not affect in excess to the production of capsules, as it is described in the introduction, so to avoid an instability of the chain of droplets that drop from the nozzle an average amplitude of vibration is fixed, with a value of 6.

Table 2. Parameters which were kept constant during the optimization process

Parameter	*Assigned Value*
Air pressure	400 mbar
Electrode voltage	350 V
Amplitude of vibration	6
Sodium alginate concentration	1% w/v
Calcium chloride concentration	1% w/v
Nozzle diameter	750 μm

4.2.2 Procedure to set the working range

The first part of the work is to establish the working range with the selected sodium alginate solution (1%).

For this purpose, a position of the valve is set at a minimum frequency in which a continuous chain of droplets [Fig. 8] leaving the nozzle is seen, as the Buchi manual recommends, and capsules are obtained, verifying by eye that they are spherical.

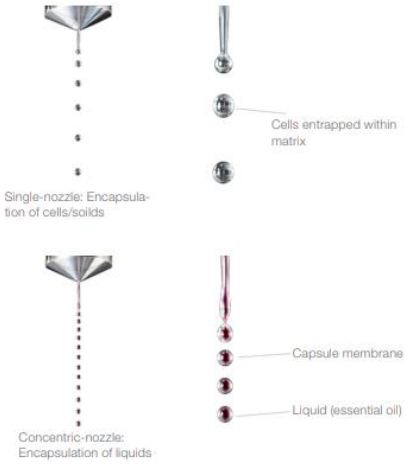

Figure 8. Chain of spheres (From BUCHI Labortechnik, 2016)

In the case that the obtained capsules are not spherical, these parameters are not acceptable and in this way the range is narrowed to guarantee an acceptable result. The complete ranges are from 0 to 9 for the position of the valve, 9 being the closed valve position and 0 the most open position; and between 80Hz and 2000Hz the values of the frequency. For each design, the ranges shown in the Tables 3 have been obtained.

Then begin to work at a pressure of 400 mbar in which the range was applied. The values obtained were the following:

Table 3. Range of frequency and flow rate valve position opening for the study

Frequency (Hz)	Range of valve position opening
100	8 – 3,5
200	8 – 4,5
300	6 – 4,5
400	8 – 3
500	8 - 5

As can be seen in the Table 4, the common valve opening range for all frequencies is 4.5 to 6 turns. In this range, the capsules come out all spherical by eye although there is a size distribution.

Table 4. Variables and levels selected

Variable	Low level	High level
Frequency	145	355
Valve position	4,75	5,75

In the Table 4 the variables and levels considered for programming the experimental design are shown. The selected levels have been obtained experimentally as described above.

The values chosen as maximum and minimum are not those of the working range for the factorial design, because for the composite central design rotation is required that extends the range and eventually extends range. When rotating the factors, the range cannot be exceeded, and to guarantee that the ends of the rotation are the established ones of the range, the values of the design are reduced to two levels, taking those of the previous table.

4.3 TWO-LEVEL FACTORIAL DESIGN: INFLUENCE AND EFFECTS OF THE VARIABLES

It is important to know how the different variables influence the process, in order to predict and justify the responses resulting from the experimental design created.

4.3.1 Interactions between variables

The factorial design allows to obtain different graphs showing the variation of capsule diameter, standard deviation, flow rate and sphericity (response variables) for the upper and lower levels of two variables studied (factors), keeping the other two variables constant and, thus, observe the presence or absence of interactions.

In the first part of this study, a complete 2x2 factorial design was used to see the main effects and interactions on the two input variables (valve frequency and position). For them, the different answers (flow rate, beads diameter, standard deviation and sphericity) are studied and analysed in order to check whether or not they can be studied independently.

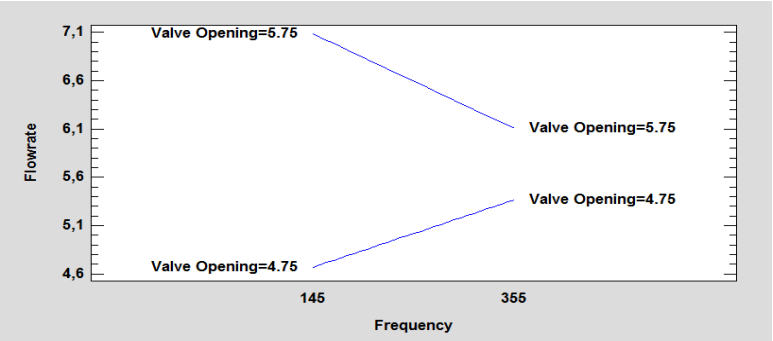

Figure 9. Interaction for flow rate.

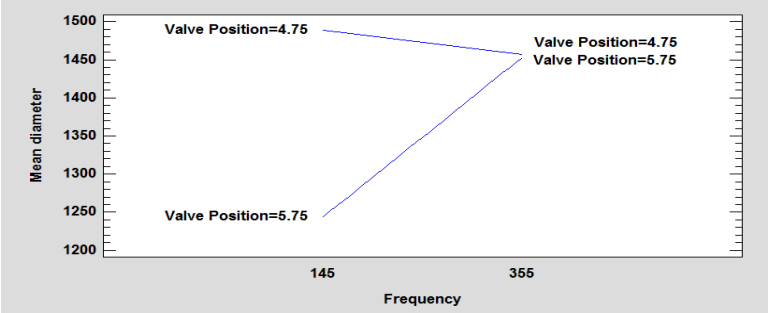

Figure 10. Interaction for mean diameter.

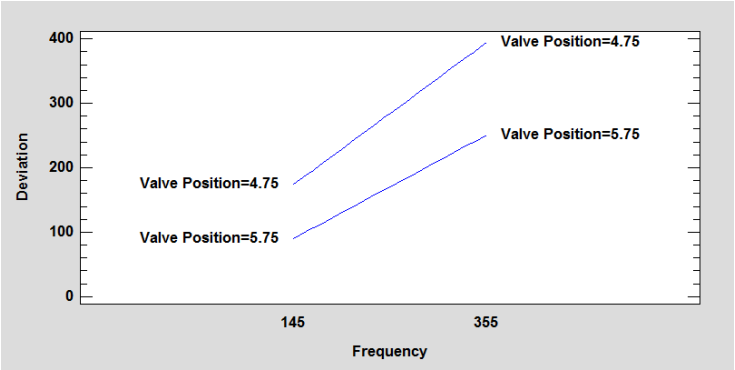

Figure 11. Interaction for standard deviation.

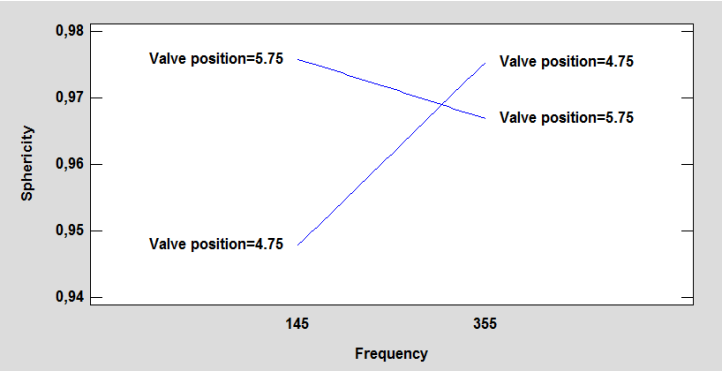

Figure 12. Interaction for sphericity.

As shown in Figures 9,10,11 and 12 for each response variable there is interaction. The response variable that seems to have a greater interlace of variables is the sphericity, followed by the diameter, the flow rate and finally the standard deviation of size distribution. The latter has non-parallel lines, which is interaction but not a very high one.

Therefore, it can be concluded that the value of one factor (frequency or position of the valve) has an influence on the response when the other factor is changed, and therefore these variables cannot be studied independently, but together. Based on these interferences, a central composite design of two factors, valve position and frequency (CCD) with three runs of the central point will be carried out, with a total of 11 experiments, in order to obtain a response surface, inside the experimental range previously determined.

4.3.2 Central composite design for two factors

A full design, two-factor level Central Composite Rotatable Design (CCRD) (Montgomery, 2001) was used to optimize the alginate bead production using the BÜCHI-390 Encapsulator. Two independent variables, namely frequency (X_1) and flow rate valve opening position (X_2), were studied at two levels. The CCRD was composed of 4 high/low factorial combinations (coded ±1,), 4 very high/very low axial points combinations (coded $\pm\alpha$, where α is equal to 1,41 for a circumscribed CCRD, as discussed in introduction, and 3-time replicated central point (coded 0) combinations. Factor settings in each of the CCRD combination was determined using the software StatGraphics Centurion XVII (StatGraphics Technologies, Inc., Virginia, USA) based on the variable ranges (low to high values) supplied to the software. The ranges ($-\alpha$,$+\alpha$) for frequency (100 to 400 Hz) and valve opening position (4,5 to 6) supplied to the software was based on the preliminary work that involved a modified COST analysis (as described previously), and as supported by related literature. Figure 13 represents values of input variables.

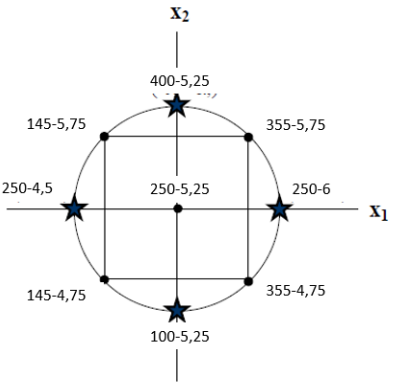

Figure13. Values of factors for the Central Composite Rotatable Design

A complete CCRD experiment design allows estimation of a full quadratic model for each of the four responses, namely, flow rate (Y_1), mean diameter of the alginate beads (Y_2), standard deviation of the mean diameter of the beads (Y_3), and spherical factor of the beads, calculated as lower radius/larger radius for each -presumably elliptical- bead (Y_4).

Table 5. Experimental conditions according to the inscribed CCRD and response value parameters

Run order	*Coded variables*		*Uncorded variables*		*Response*			
	Frequency (Hz) (X_1)	Valve opening position (X_2)	*Frequency (Hz) (X_1)*	Valve opening position (X_2)	*Mean diameter (Y_1) (µm)*	*Flow rate (Y_2) (ml/s)*	*Standard deviation (Y_3)*	*Sphericity (Y_4)*
1	- α	0	100	5.25	1283.14	0.5648	224.42	0.9766
2	-1	-1	145	4.75	1488.18	0.7082	174.29	0.9478
3	+1	-1	145	5.75	1244.16	0.4672	90.36	0.9759
4	0	- α	250	4.5	1532.45	0.8099	72.77	0.9857
5	0	+ α	250	6	1048.04	0.5391	87.59	0.9737
6	+1	-1	355	4.75	1456.66	0.6104	394.45	0.9754
7	+1	+1	355	5.75	1453.16	0.5366	250.66	0.9669
8	+ α	0	400	5.25	1345.6	0.6576	237.2	0.9768
9	0	0	250	5.25	1014.86	0.6475	82.54	0.9602
10	0	0	250	5.25	1003.66	0.6016	89.62	0.9820
11	0	0	250	5.25	1012.29	0.6524	85.78	0.9882

The data of the Table 5 for the 11 experiments have been obtained following the process explained below:

The data of Table 5 for the 11 experiments have been obtained as follows:

Each experiment is performed to obtain loosely more than 400 capsules. Before obtaining the capsules, the flow is measured three times to obtain a reproductible, stable result. When the capsules are formed, they are filtered, and several photographs [Figure 14] are taken using the Optika microscope to later measure the diameter of 400 capsules and make the data treatment. When capsules were non-spherical, higher and lower diameters are measured in order to obtain sphericity, calculated as quotient of the lower diameter and the higher diameter. The diameters are used to perform the histograms [Figure 15].

The histograms are adjusted following a logarithmic-normal distribution which picks up and extrapolates all the data more optimally.

Figure 14. Image of alginate capsules

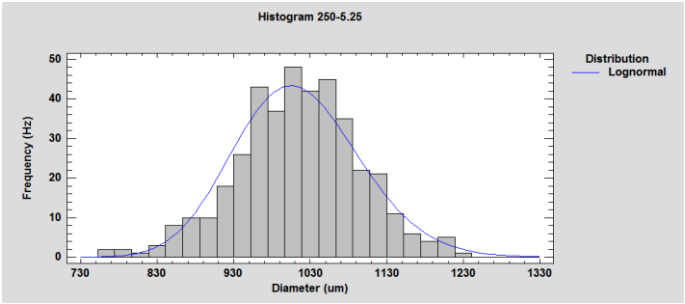

Figure 15. Histogram of 250 Hz and 5.25 valve position. Line: log-normal fitting.

4.3.3 Treatment of experimental results

The Pareto Diagram shows the estimated effects and interactions, positive or negative, in order of importance. The vertical line represents the value from which some effects and interactions become significantly important, i.e. the effect is higher than experimental error, with a 95% of probability. Therefore, the effects and interactions that exceed the line are significantly important with a 95% probability.

In Figure 16, the response values of the bead diameter obtained experimentally are shown and using the Statgraphic Centurion XVII program, the Pareto diagrams of Figure 17 are obtained.

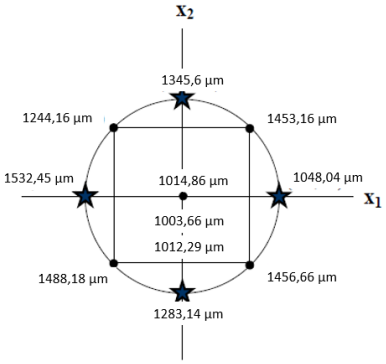

Figure 16. Experimental design and the measured values for mean diameter

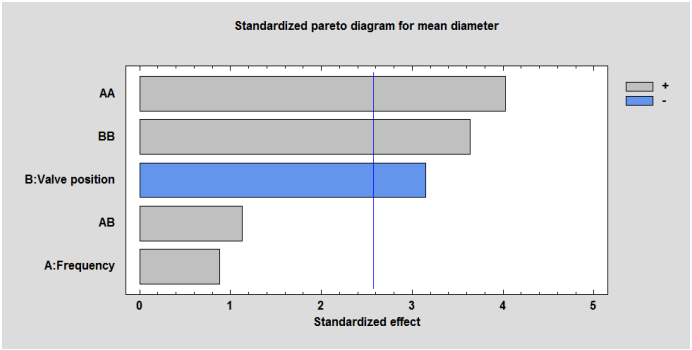

Figure 17. Standardized Pareto diagram for mean diameter

For the standard deviation and the sphericity there is no significant influence of any of the input variables into the range tested while for the diameter some factors and some interactions influence the response variable.

The Pareto graph of the standardized effect for the mean diameter of the cord [Figure 16] indicates that valve position, square of frequency and square of valve position affect mean bead diameter with 95% confidence. Therefore, all these terms must be considered in the empirical equation.

For flow rate only, the valve position is statistically significant (Pareto diagram in Annex 1), so that only this variable will appear in the empirical equation. In the responses of the standard

deviation and the sphericity the effects extend within this reference line, so they are statistically insignificant. For these two response variables, we do not obtain an empirical equation, but an average of the experimental results obtained. The rest of the diagrams are included in Annex 1.

The coefficients and their confidence intervals are obtained with a total error of 10 degrees of freedom.

Table 6. Mean coefficients for each response

Effect/Response	Coefficient	Confidence Interval (95%)
Standard Deviation of bead diameter (-)	162,72	± 69,68
Sphericity of beads (-)	0,9735	± 0,0078

The response surface equations to predict mean bead size and flow rate were obtained according to the CCD and variable input, with their respective confidence intervals with a 95% probability for each of the parameters involved in the equation, as shown in Equations 5 and 6 and Tables 7 and 8.

$$Bead\ diameter = (19598 \pm 145) - (8 \pm 191) * \text{Frequency(Hz)} - (6464 \pm 187) * \text{Valve position}(-) + (0{,}0161 \pm 228) * \text{Frequency}^2 + (594 \pm 193) * \text{Valve position}^2 \quad \text{[Eq 5]}$$

Table 7. Analysis of Variance (ANOVA) for the bead diameter

Source of Variation	Sum of Squares	Dj[a]	Mean Square	F-Value	P-value
Valve position (-) (X_1)	111640	1	111640	9,82	0,0165*
Square of frequency (Hz^2) $(X_2)^2$	182424	1	182424	16,05	0,0051*
Square of valve position (-) $(X_1)^2$	149162	1	149162	13,12	0,0085*
Pure error	79566	7	11367		
Total (corr.)	442441	10			
R^2	82,02%				
Adjusted R^2	74,31				

*Statistically significant at p= 0,05

[a]Degrees of freedom

$$Flow\ rate = (1{,}5084 \pm 0{,}03679) - (0{,}1697 \pm 0{,}08372) * Valve\ position \quad \text{[Eq. 6]}$$

Table 8. Analysis of Variance (ANOVA) for the bead diameter

Source of Variation	Sum of Squares	Dj[a]	Mean Square	F-Value	P-value
Valve position (-) (X_1)	0,0611631	1	0,0611631	21,01	0,0013 *
Pure error	0,0261963	9	0,0261963		
Total (corr.)	0,0873594	10			
R^2	70,01%				
Adjusted R^2	66,68				

*Statistically significant at p= 0,05

[a]Degrees of freedom

Since p-values of the variables are all less than the level of significance (0.05), it can be concluded that the effects of these terms on the mean bead are statistically significant.

The correlation coefficient R^2 refers to the percentage of variation (0 to 100%) in the response that is explained by the model. The higher the R^2 value, the better the model fits the data (Gabriel, 2008). In both cases, mean diameter and flow rate, the correlation coefficient has a high value, so the model fits correctly.

Before showing the response surface the residual graph is observed. The residual graphs are used to verify if the model fits well or not. If the distribution of residues is random, it can be concluded that no tendencies are observed in the model.

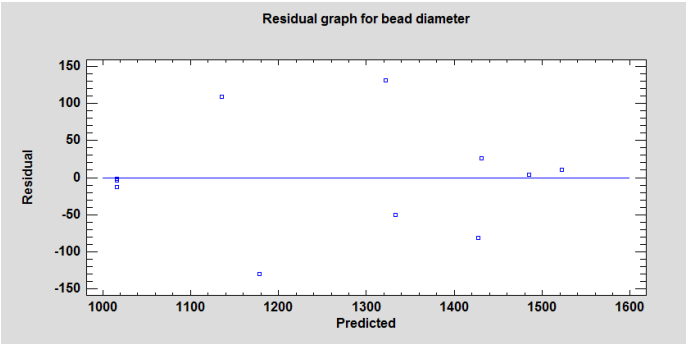

Figure 18. Residual graph for bead diameter.

As it is observed in the residual graph [Figure 18], it does not show any tendency since residues follow a random distribution, which is an indication that response surface might be a good fitting for prediction of results. The rest of residual graphs for the different answers are shown in Annex 1, all of them do not show tendencies obtaining a random distribution giving a good adjustment to the obtained model. The response surface obtained with the experimental design in the range studied is shown in Figure 19.

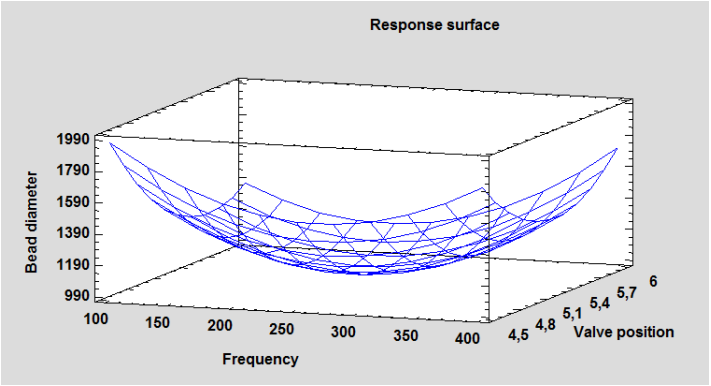

Figure 19. Response surface plot of bead diameter.

When charted on a 3-dimensional plot, the response surface shown has a curved shape because the model contains quadratic terms that are statistically significant.

Figure 19 shows the response surface obtained for the bead diameter in which the diameter is observed as a function of the input variables.

The response surface is curved due to the quadratic term of the frequency and the position of the valve. The greater the value of the valve position (lower flow rate), the greater the loss of load since the passage section narrows obtaining a smaller flow rate and therefore a smaller droplet size. At higher frequency values, the flow of passage is cut into smaller droplets so that smaller droplet sizes are observed.

For flow rate [Figure 20] the response surface has a flat shape because the model that describes it is linear.

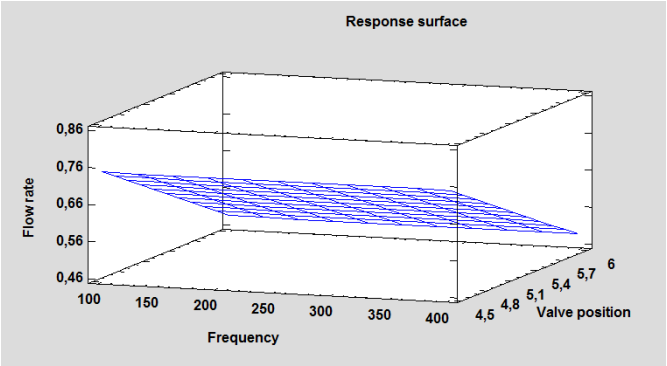

Figure 20. Response surface plot of flow rate.

In the graph it is observed how for smaller valve positions a greater flow is obtained. The frequency does not significantly influence the response.

4.3.4 Model validation using confidence and prediction intervals

A predictive model may only be safely used in decision making when validated. Validation is an essential step that reveals the applicable range of a model and the limits of its performance (Gabriel, 2008).

Therefore, to validate the predictive model equations generated for mean bead diameter and flow rate, validation experiments were done using a set of data obtained from additional test runs, independent from those performed in the elaboration of the model.

Confidence intervals are used to indicate the amount of uncertainty or imprecision around the effect size calculated, using the study sample to estimate the true effect size in the source population. Confidence interval takes into account sampling error; the effect size and its confidence interval represent plausible values for the source population (Patino & Ferreira, 2015). Prediction bands show the variation or scatter in the data.

The obtained values of the bands are obtained by means of equations 7 and 8.

$$Confidence\ interval = \mathrm{Yi} \pm \mathrm{s.e} * \sqrt{\frac{1}{n} + \frac{(xi - \bar{x})^2}{SSxx}} \qquad \text{Eq [7]}$$

$$Predicted\ interval = \mathrm{Yi} \pm \mathrm{s.e} * \sqrt{1 + \frac{1}{n} + \frac{(xi - \bar{x})^2}{SSxx}} \quad \text{Eq [8]}$$

Where:

$s.e = \sqrt{\frac{SS}{n-\alpha}}$

$SSxx = \sum(xi - \bar{x})^2$

n = number of experiments

n – α = freedom degrees

The experiments carried out are shown in Table 9.

Table 9. Experiments for the validation of the CCD design.

Run	Frequency (Hz)	Valve position
1	180	5
2	230	5
3	300	5
4	200	4,5
5	200	5
6	200	5,5

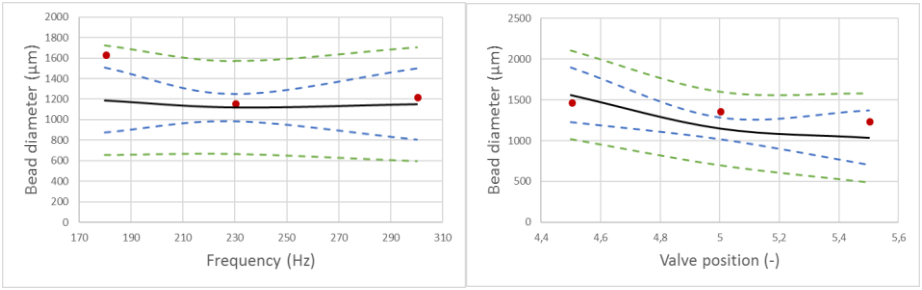

Figure 21. Validation for bead diameter.

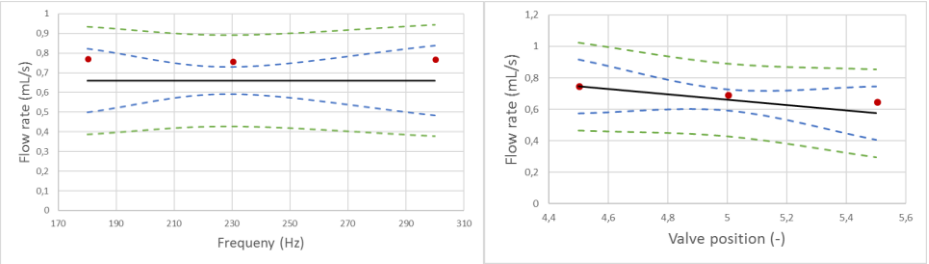

Figure 22. Validation for flow rate.

Figures 21 to 22 show validation experiments together to surface response cuts maintaining valve position or frequency, with the corresponding confidence interval. Although results are inside the range, all validations show a slight tendency toward values higher than expected.

As all the validations have the same tendency, it was though that probably some uncontrolled variable changed from one set of experiments, made for the CCD, to the other, made for validation. Some weeks passed between both sets, temperature of feeding bottle was not controlled, and the first set of experiments was done in days where environmental temperature was especially low. We suspected that it could have affected the viscosity of the alginate solution and, therefore, the pressure drop along the system, so the flow rate and the bead size were affected. In order to quantify how much temperature affected viscosity of alginate solution, steady state viscosity vs. shear rate was determined for 1% sodium alginate solutions at different temperatures.

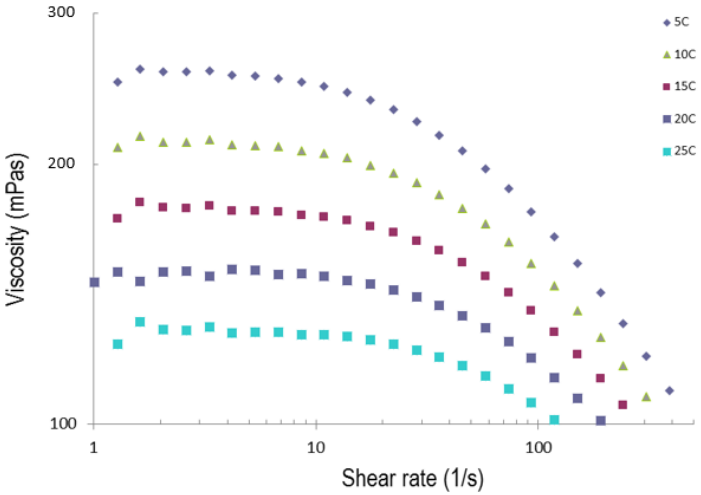

Figure 23. Viscosity test of sodium alginate 1% at different temperatures.

As it can be seen in Figure 23, the viscosity of the alginate used in the experimental design decreases significantly when temperature is increased. As validation was carried out in warmer days when experimental design, alginate solutions presumably presented lower viscosities. Then, a slightly higher flow rate was obtained with the same valve position, resulting, moreover, in slightly higher bead diameters. On the other hand, alginate solutions were stored in fridge and taken out and used directly without attempter, so temperature probably changed from the first to the last experiment along the same day.

For this reason, it was decided to carry out a second experimental design in which temperature was controlled and maintained at 25ºC.

4.4 EXPERIMENTAL DESIGN AT 25 DEGREES

This experimental design was carried out following the same steps than the previous one, with the only difference that the alginate used by the Buchi encapsulator was submerged in a thermostatic bath of water at 25ºC.

4.4.1 Establishing the experimental range

When modifying the temperature, the viscosity of the sodium alginate is modified, so the new working range must be determined experimentally again. The procedure to be followed is the same as that described for the first design.

The new working range is shown in Table 10.

Table 10. Range of frequency and flow rate valve position opening for the study.

Frequency (Hz)	Range of Flow Rate Valve Position
100-300	6 - 8

The same as what happened with the previous design, as it is a rotational design, the maximum and minimum ranges established for the two-level factorial design are smaller to guarantee never leaving the maximum perimeter [Table 11].

Table 11. Variables and levels selected.

Variable	Low level	High level
Frequency	130	270
Valve position	6,25	7,75

It is observed that the range has moved to higher valve positions, corresponding to more closed valve. It was expected, since higher temperature implies lower viscosity, more ease of passage and more flow rate can circulate. The frequency, however, was just slightly modified.

Figure 24 shows the values of the combined obtained range of each experiment.

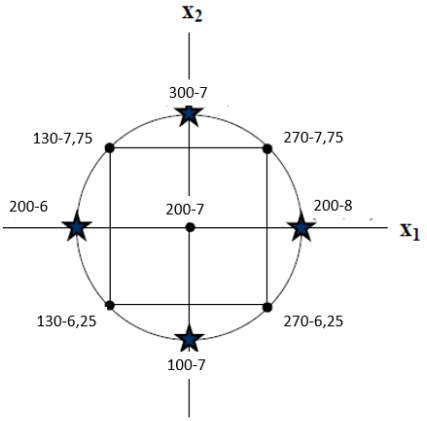

Figure 24. Response values for the Central Composite Rotatable Design for 25ºC.

Table 12. Experimental conditions according to the inscribed CCRD and response value parameters for 25ºC.

Run order	*Coded variables*		*Uncorded variables*		*Response*			
	Frequency (Hz) (X_1)	Valve opening position (X_2)	*Frequency (Hz) (X_1)*	Valve opening position (X_2)	*Mean diameter (Y_1) (μm)*	*Flow rate (Y_2) (ml/s)*	*Standard deviation (Y_3)*	*Sphericity (Y_4)*
1	+1	-1	270	6,25	1638,08	0,7668	137,83	0,9270
2	0	0	200	7	1614,57	0,9457	115,89	0,9283
3	+α	0	300	7	1386,68	0,5969	189,17	0,9978
4	0	0	200	7	1616,03	0,9729	88,25	0,9865
5	-1	-1	130	6,25	1931,46	1,0762	119,27	0,9840
6	-α	0	100	7	1868,32	0,9534	94,81	0,9801
7	0	+α	200	8	990,965	0,5435	73,44	0,8827
8	0	-α	200	6	1489,64	0,9922	172,35	0,8770
9	+1	-1	130	7,75	1424,44	0,6916	115,07	0,9344
10	0	0	200	7	1591,61	0,9013	119,76	0,6880
11	+1	+1	270	7,75	1323,42	0,9046	181,59	0,8985

Following the same procedure as in the previous design, each one of the response variables is measured as before, with the Statgraphic Centurion XVII program and the Optika magnifying glass, obtaining the results shown in Table 12.

4.4.2 Treatment of experimental results

For all the response variables studied (diameter, flow rate, standard deviation and sphericity) the corresponding Pareto diagram is obtained with 95% confidence in which it is observed which factors significantly affect responses. Factors that exceed the vertical line, which indicates the limits of changes due to experimental error, will have a statistically significant influence. On the contrary, those that do not exceed this line will not have a significant influence.

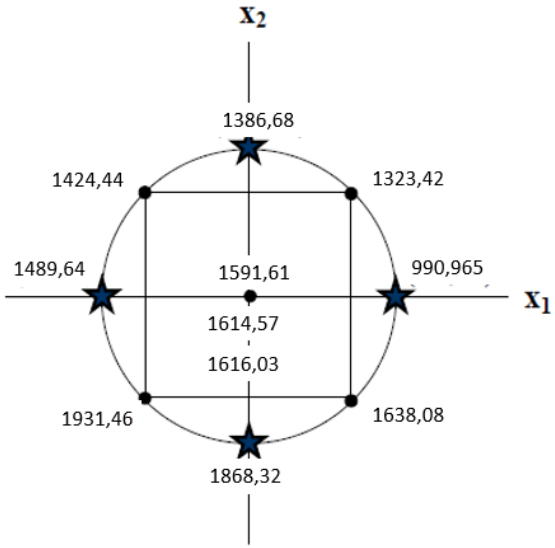

Figure 25. Experimental design and the measured values for mean diameter with a temperature of sodium alginate at 25 ° C.

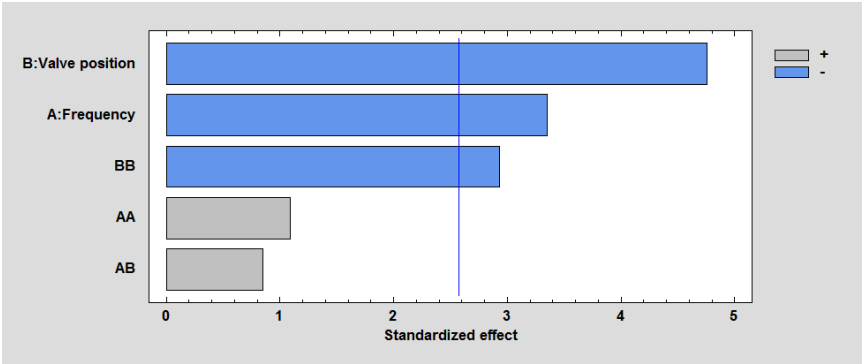

Figure 26. Standardized Pareto diagram for mean diameter for 25ºC.

Figure 25 shows the mean diameter values obtained experimentally and in Figure 26 the Pareto diagram for the mean diameter is shown. The factors that influence mean diameter are frequency, valve position and squared valve position. Pareto diagrams for the other responses (flow rate, standard deviation and sphericity) are shown in Annex 2. In the case of the flow rate, only the valve position influences the results, with a significance of the 95%, while for the standard deviation and the sphericity input variables do not affect response ones in the range tested. For these two last cases, therefore, a mean value is just obtained, with the corresponding confidence interval for 10 degrees of freedom [see Table 13]. The coefficients and their confidence intervals are obtained with 10 degrees of freedom.

Table 13. Mean coefficients for each response

Effect/Response	Coefficient	Confidence Interval (95%)
Standard Deviation (-)	127,95	± 25,84
Sphericity (-)	0,9168	± 0,0585

The response surface equations to predict mean bead size and flow rate were obtained according to the CCD and input variables, with their respective confidence intervals with a 95% probability for each of the parameters involved in the equation, as shown in Equations 9 and 10 and Tables 14 and 15.

$$Bead\ diameter = (-10793{,}6 \pm 114) - (2 \pm 188) * \text{Frequency} + (3927 \pm 194) * \text{Valve position} - (299 \pm 236) * \text{Valve position}^2 \quad \text{Eq [9]}$$

Table 14. Analysis of Variance (ANOVA) for the bead diameter.

Source of Variation	Sum of Squares	Dj[a]	Mean Square	F-Value	P-value
Valve position (-) (X_1)	292489	1	292489	11,38	0,0119*
Frequency (Hz) (X_2)	144985	1	144985	22,96	0,0020*
Square of valve position $(X_1)^2$	145375	1	145375	11,41	0,0118*
Pure error	89172	7	12738		
Total (corr.)	672022	10			
R^2	86,73%				
Adjusted R^2	81,04				

*Statistically significant at p= 0,05

[a]Degrees of freedom

$$Flow\ rate = (1{,}8934 \pm 0{,}1036) - (0{,}1491 \pm 0{,}2450) * valve\ position \quad \text{Eq [10]}$$

Table 15. Analysis of Variance (ANOVA) for the bead diameter.

Source of Variation	Sum of Squares	Dj[a]	Mean Square	F-Value	P-value
Valve position (-) (X_1)	0,09451	1	0,09451	4,10	0,0736 *
Pure error	0,2075	9	0,02305		
Total (corr.)	0,3020	10			
R^2	31,30%				
Adjusted R^2	23,66				

*Statistically significant at p= 0,05

[a]Degrees of freedom

For the flow rate there is a poorer adjustment than for the mean diameter, since for the mean diameter the R^2 is 86,73 while for the flow rate it is 31,20.

Before showing the response surface the residual graph is observed.

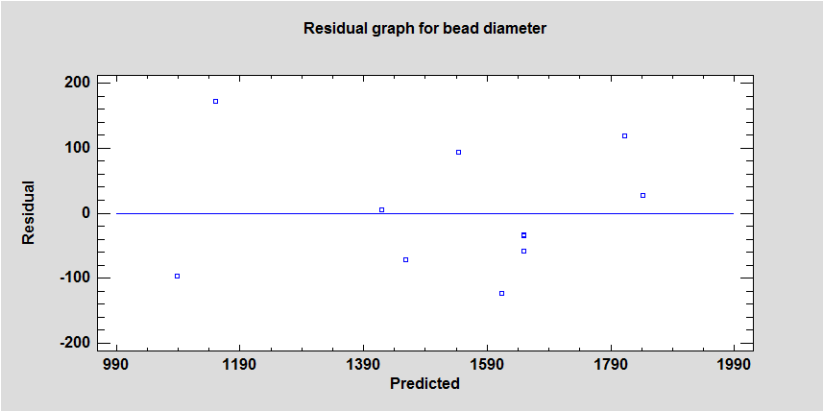

Figure 27. Residual graph for bead diameter for 25ºC.

As it is observed in the residual graph [Figure 27], it does not show any tendency since residues follow a random distribution, which is an indication that response surface could be a good fitting for prediction of results.

The response surface obtained for the bead diameter with the experimental design in the range studied is shown in Figure 28.

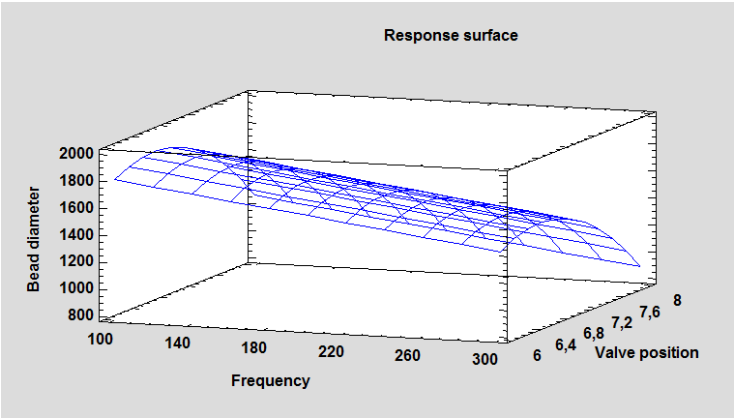

Figure 28. Response surface plot of bead diameter for 25ºC.

As seen in the Figure 28 the lower frequencies and the lower valve positions (more opened valve), the higher the bead diameter, although a curvature of the surface in the direction of the valve position is observed due to the influence of the quadratic term. This is attributed to the fact that when the valve is more opened, the pressure drop crossing it is lower and, therefore, the mass flow increases, according to Bernouilli equation.

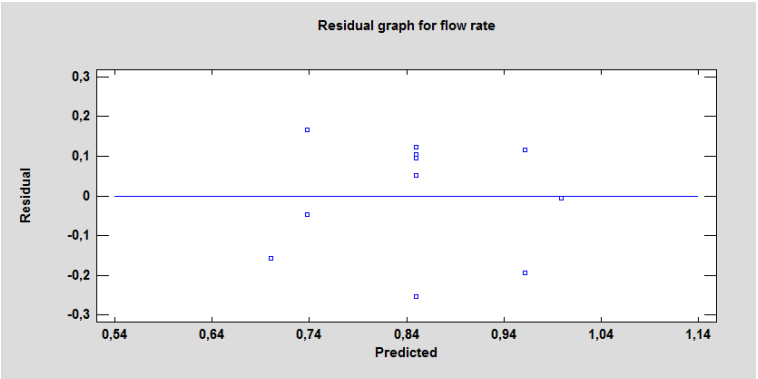

Figure 29. Residual graph for flow rate for 25ºC.

Figure 29 shows the residual graph for the flow rate, it does not show any tendency since residues follow a random distribution, which is an indication that response surface might be a good fitting for prediction of results. The other residual graphs can be seen in Annex 2.

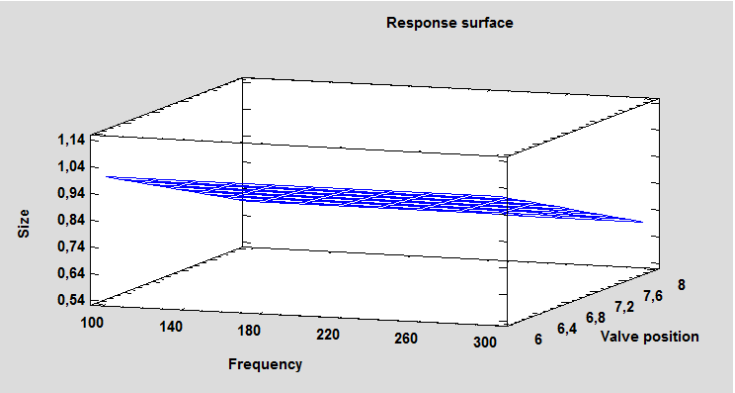

Figure 30. Response surface plot of flow rate for 25ºC.

In Figure 30 it can be observed that the response surface has a flat shape because the model that describes it is linear. This is because the equation obtained in the model is linear, in which only that variable influences, thus obtaining the flat surface.

4.4.3 Model validation using confidence and prediction intervals

Therefore, to validate the predictive model equations generated for the mean value and flow rate, validation experiments were done using a set of data obtained from additional tests, carried out independently from those performed in the elaboration of the model.

The experiments carried out are shown in Table 16.

Table 16. Experiments for validation.

Run	Frequency (Hz)	Valve position
1	150	7,25
2	220	7,25
3	250	7,25
4	180	6
5	180	6,5
6	180	7

Using the equations 7 and 8 and the values obtained in the validation of the answers that have significant influences (bead diameter and flow rate), the validation study is carried out.

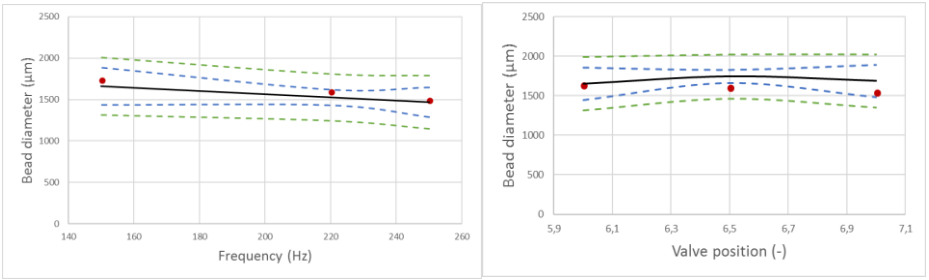

Figure 31. Validation for bead diameter.

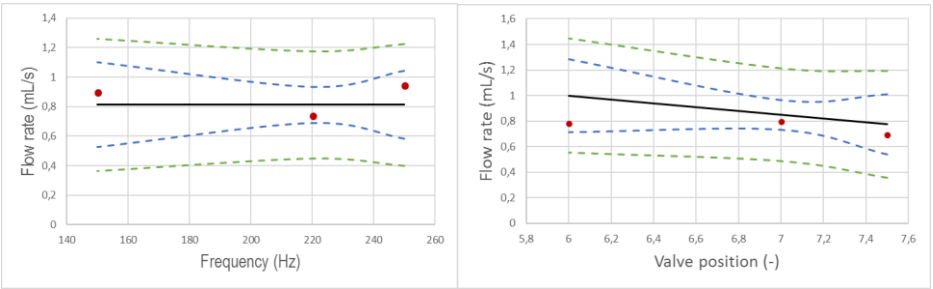

Figure 32. Validation for flow rate.

Figures 31 to 32 show validation experiments together to surface response cuts maintaining valve position or frequency, with the corresponding 95% confidence interval.

All the experiments are within the interval of confidence intervals. No trends were observed in the deviations of the predicted values through the equation obtained in the central composite design (CCD), so we can conclude that the design studied is good.

5. CONCLUSIONS

The conclusions that can be derived from this work are the following:

- It has been found a range of work for valve position and frequency within which it is possible to obtain beads visually spherical (by eye).
- The results of the flow rate are independent of the person who places the position of the valve, while the mean size of the beads obtained in the count of the same photograph is strongly influenced by who measures the capsules of the images, therefore to avoid errors, they must be measured by the same person.
- The population size must be at least 400 beads to guarantee significant results.
- The input variables interact with each other and therefore they must be studied together in the experimental design that considers these possible interactions, such as the CCD.
- The temperature of the hydrocolloid that must pass through the equipment must be controlled, because it affects the viscosity and therefore the pressure drop and the flow rate and in turn the size of formed beads.
- Through the CCD, response surfaces are obtained that can reasonably estimate the response variables (flow rate, bead diameter, standard deviation and sphericity).
- The sphericity and the standard deviation are independent of the input variables (frequency and valve position) within the range studied.
- The flow rate varies linearly with the position of the valve increasing when valve opens due to the decrease in the pressure drop and it is independent of the frequency within the range studied.
- The bead diameter is significantly influenced by the frequency, the position of the valve and the position of the valve squared, decreasing when frequency is increased because it cuts the flow more frequently and therefore in smaller drops. When the position of the valve is increased and, therefore, lower flow rates are obtained, smaller beads are formed.

When making extra experiments independent to the experimental design ones, results are obtained within the confidence interval of the response surface, which allows to validate the model obtained.

REFERENCES AND NOTES

Anal, Anil Kumar and Singh, Harjinder. Recent advances in microencapsulation of probiotics for industrial applications and targeted delivery. Trends in Food Science & Technology. 2007, 18:240-251.

Borgogna, M.; Bellich, B.; Zorzin, L.; Lapasin, R. and Cesàro, A. Food microencapsulation of bioactive compounds: rheological and thermal characterisation of non-conventional gelling system. Food Chemistry. 2010, 122(2):416-423.

Brandenberger, H., Nussli, D., & Widmer, F. Monodisperse particle production: A method to prevent drop coalescence using electrostatic forces. *Journal of Electrostatics,* 1999, *45*(3), 227-238.

BUCHI Labortechnik AG. Operation Manual (Original) Encapsulator B-390. Flawil, Swirzerland: BUCHI Labortechnik AG, 2016, May.

Champagne, Claude P. and Fustier, Patrick. Microencapsulation for the improved delivery of bioactive compounds into foods. Current Opinion in Biotechnology. 2007, 18(2):184-190.

Chan, Eng Seng; Lee, Boon Beng; Ravindra, Pogaku and Poncelet, Denis. Prediction models for shape and size of ca-alginate macrobeads produced through extrusion-dripping method. Journal of Colloid and Interface Science. 2009, 338(1):63-72.

Deladino, Lorena; Anbinder, Pablo S.; Navarro, Alba S. and Martino, Miriam N. Encapsulation of natural antioxidants extracted from *Ilex paraguariensis*. Carbohydrate Polymers. 2008, 71(1):126-134.

Draget, K.I. Alginates. In Handbook of hydrocolloids. (pp. 379-395). Cambridge, England: Woodhead Publishing Limited - Boca Raton, 2000, FL, USA: CRC Press LLC.

Feng Peng, Z., Satrack, D., Baumert, A., Subramaniam, R., Goh, N. K., Chia, T. F., et al. Antioxidant flavonoids from leaves of Polygonum hydropiper L. Phytochemistry, 2003, 62(2), 219e228.

Funami, Takahiro; Fang, Yapeng; Noda, Sakie; Ishihara, Sayaca; Nakauma, Makoto; Draget Kurt I. Nishinari, Katsuyoshi and Phillips, Glyn O. Rheological properties of sodium alginate in an aqueous system during gelation in relation to supermolecular structures and Ca2+ binding. Food Hydrocolloids. 2009, 23(7):1746-1756.

Fundueanu, G., Nastruzzi, C., Carpov, A., Desbrieres, J., & Rinaudo, M. Physico-chemical characterization of Ca-alginate microparticles produced with different methods. *Biomaterials,* 1999, *20*, 1427-1435.

Gabriel, A. Estimation of water activity from pH and Brix values of some food products. *Food Chemistry,* 2008, *108*, 1106-1113.

García, E., Saucedo, I., Navarro, R., Dzul, M., del Pilar González, M., Elorza, E., & and Guibal, E. Encapsulation of Cyanex 302 with Alginate for Palladium Recovery. *Macromol. Symp.,* 2017, *374*, 1600135.

Goh, C. H., Heng, P.W. S., & Chan, L.W. Alginates as a useful natural polymer for microencapsulation and therapeutic applications. Carbohydrate Polymers, 2012, 88(1), 1e12.

Helgerud, Trond; Gåserød, Olav; Fjæreide, Therese; Andersen, Peder O. and Larsen, Christian K. Alginates. In Food stabilizers, thickeners and gelling agents. 2010, (pp. 50-72). United Kingdom: Wiley-Blackwell.

Imeson, A. Food stabilisers, thickeners and gelling agents. 2010, (1st ed.). UK: FMC BioPolymer.

Kris-Etherton, P. M., Lefevre, M., Beecher, G. R., Gross, M. D., Keen, C. L., & Etherton, T. D. Bioactive compounds in nutrition and health-research methodologies for establishing biological function: the antioxidant and anti-inflammatory effects of flavonoids on atherosclerosis. Annual Review of Nutrition, 2004, 24, 511e538.

Kukreja, A., Chopra, P., Aggarwal, A., & Khanna, P. Application of Full Factorial Design for Optimization of Feed Rate of Stationary Hook Hopper. *International Journal of Modeling and Optimization,* 2011, *1*(3), 205-209.

Kurt I. Draget, Catherine Taylor. Chemical, physical and biological properties of alginates and theirbiomedical implications, Food Hydrocolloids. 2011*, 25, 251–256*

Lupo, B. et al. Preparation of alginate microspheres by emulsification/internal gelation to encapsulate cocoa polyphenols. *Food Hydrocolloids,* 2014, *38*, 56-65.

Lopez-Rubio, A., Gavara, R., & Lagar_on, J. M. Bioactive packaging: turning foods into healthier foods through biomaterials. Trends in Food Science and Technology. 2006, 17, 5567e5575.

Mahajan, R., Gupta, V., & and Sharma, J. Comparison and Suitability of Gel Matrix for Entrapping Higher Content of Enzymes for Commercial Applications. *Indian J. Pharm. Sci.,* 2010, *72*(2), 223–228.

Mazzitelli, S., Tosi, A., Balestra, C., & Nastruzzi, C. Production and characterizayion of alginate microcapsules produced by a vibrational encapsulation device. *Journal of Biomaterials Application,* 2008, *23*, 123-145.

Milián D. J. Alginate-chitosan hydrogels: rheological and texture characterisation and improvement of walnut oil stability by concentric fluids encapsulation. 2017.

Montgomery, D. *Design and Analysis of Experiments* (5th ed.). New Jersey: John Wiley & Sons, Inc. Patino, C., & Ferreira, J. (2015). Confidence intervals: a useful statistical tool to estimate effect sizes in the real world. *J Bras Pneumol,* 2001, *41*(6), 565–566.

Owen, R. W., Giacosa, A., Hull, W. E., Haubner, R., Spiegelhalder, B., & Bartsch, H. The antioxidant/anticancer potential of phenolic compounds isolated from olive oil. European Journal of Cancer, 2000, 36(10), 1235e1247.

Pal, Kunal; Paulson, Allan T. and Rousseau, Dérick. Biopolymers in controlled-release delivery systems. In Modern biopolymer science. Bridging the divide between fundamental treatise and industrial application. 2009, (pp. 519-557). London-Burlington-San Diego: Academic Press.

Prat, X. Tort-Martorell, P. Grima, L. Pozueta. Métodos Estadísticos. Control y mejora de la calidad. 1997, Ediciones UPC.

Prior, R. L., & Gu, L. Occurrence and biological significance of proanthocyanidins in the American diet. Phytochemistry, 2005, *66(18), 2264e2280.*

Prüsse et al. Comparison of different technologies for alginate beads production. *Chem. Pap*., 2008, 62, 364-374.

Reddy-K, Ravindra and Reddy-P., Sabitha. Effect of different co-polymers on sodium alginate microcapsules containing isoniazid. International Journal of PharmTech Research. 2010, 2(4):2198-2203.

Whelehan, M. Buchi Encapsulator B-390/B-395 Pro Laboratory Guide. 2014. Flawil, Switzerland: BÜCHI Labortechnik AG.

Woodside, J. V., Young, I. S., Yarnell, J. W. G., Roxborough, H. E., McMaster, D., McCrum, E. E., et al. Antioxidants, but not B-group vitamins increase the resistance of low-density lipoprotein to oxidation: a randomized, factorial design, placebo-controlled trial. Atherosclerosis, 1999, 144(2), 419e42

APPENDICES

APPENDIX 1: FIRST DESIGN

4.3.3 Analyse the results of experimental design ANNEX 1

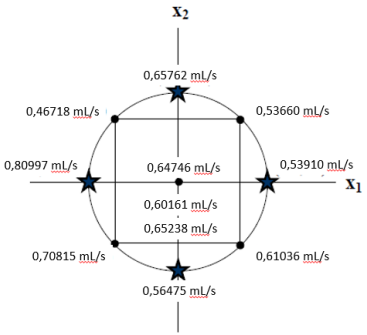

Figure 33. Experimental design and the measured values for flow rate.

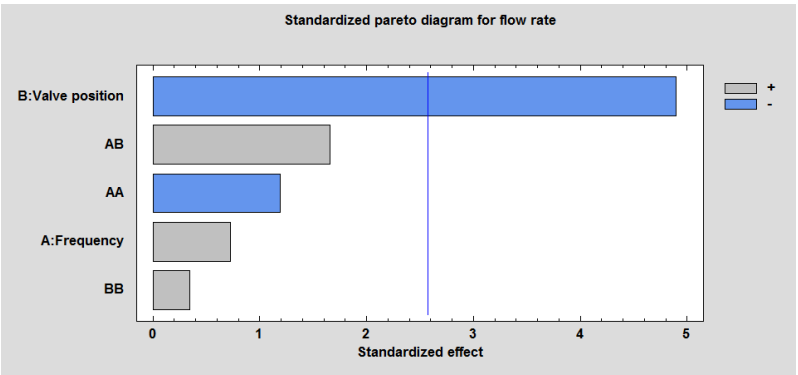

Figure 34. Standardized pareto diagram for flow rate.

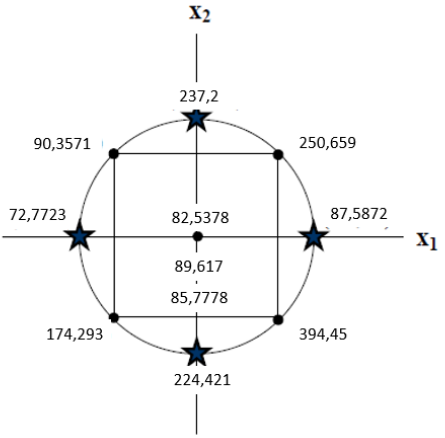

Figure 35. Experimental design and the measured values for the standard deviation of bead diameter.

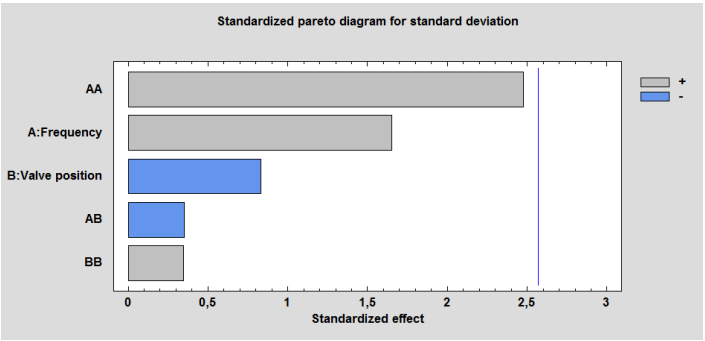

Figure 36. Standardized pareto diagram for standard deviation of bead diameter.

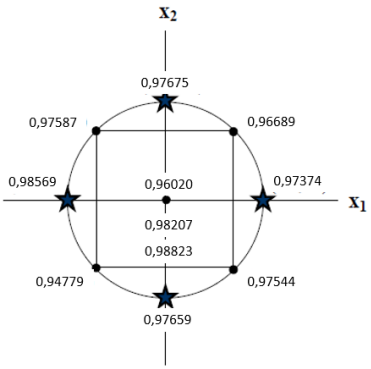

Figure 37. Experimental design and the measured values for sphericity.

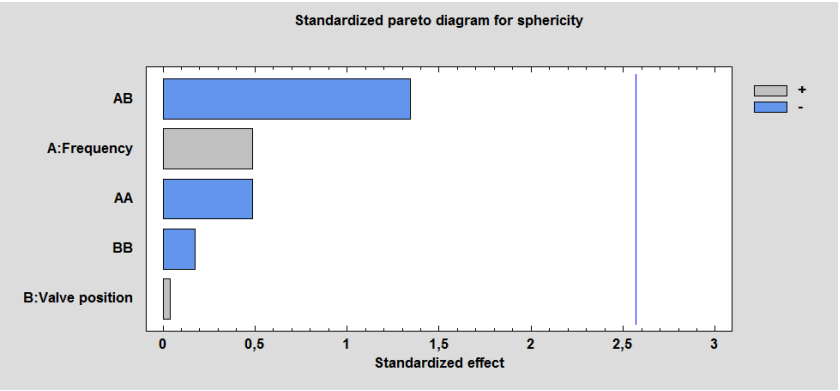

Figure 38. Standardized pareto diagram for sphericity.

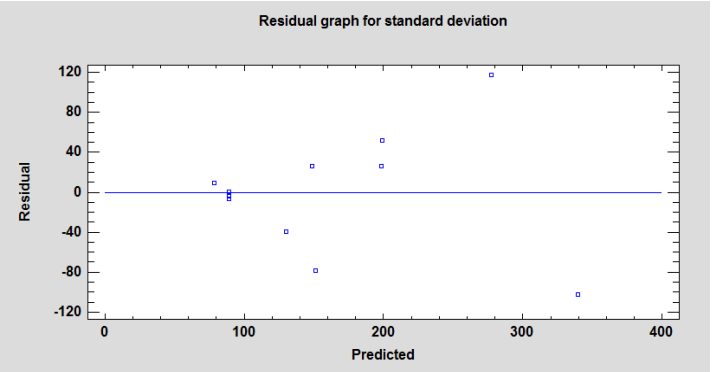

Figure 39. Residual graph for standard deviation.

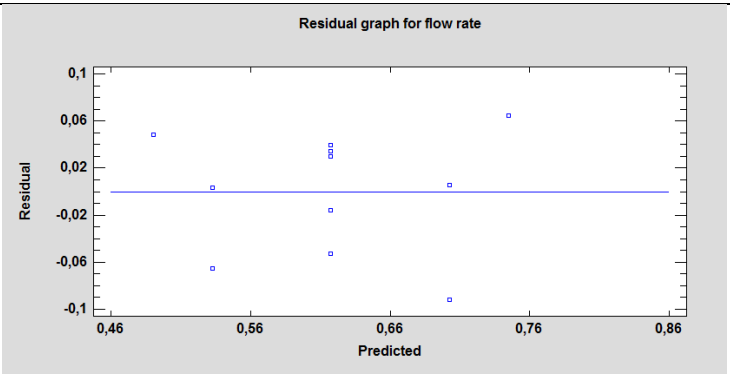

Figure 40. Residual graph for flow rate.

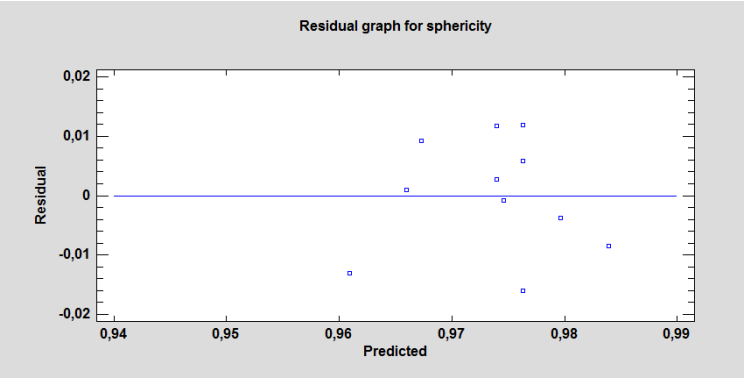

Figure 41. Residual graph for sphericity.

APPENDIX 2: SECOND DESIGN (25 DEGREES)

4.4.2 Treatment of experimental results ANNEX 2

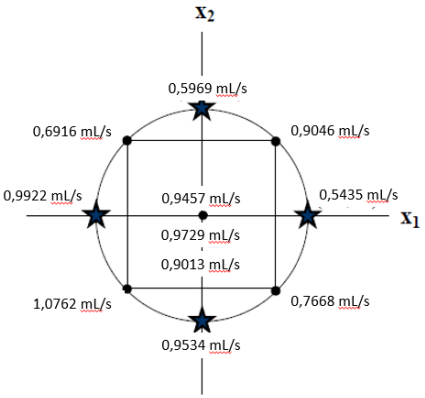

Figure 42. Experimental design and the measured values for flow rate for 25 degrees.

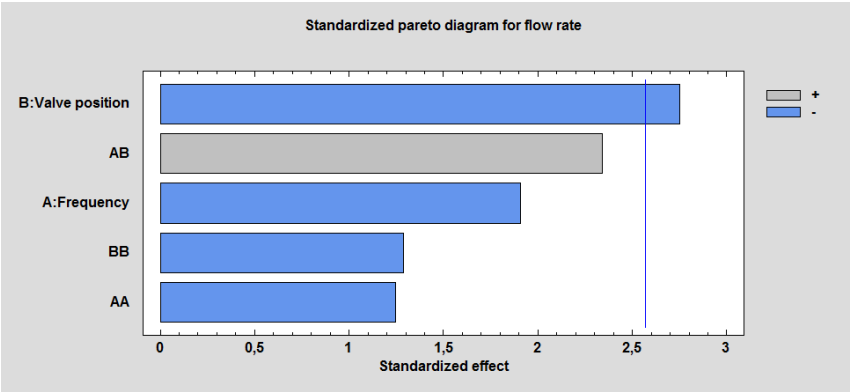

Figure 43. Standardized pareto diagram for flow rate for 25 degrees.

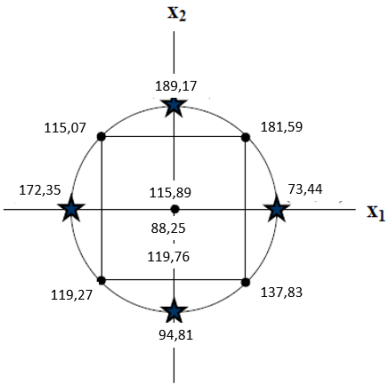

Figure 44. Experimental design and the measured values for the standard deviation of bead diameter for 25 degrees.

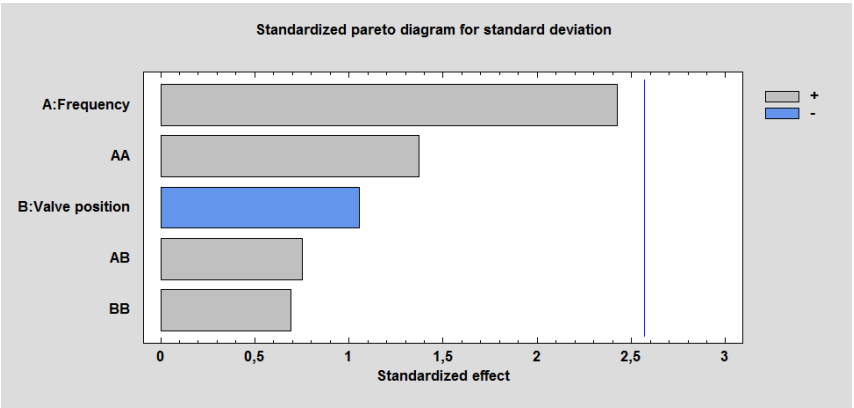

Figure 45. Standardized pareto diagram for standard deviation of bead diameter for 25 degrees.

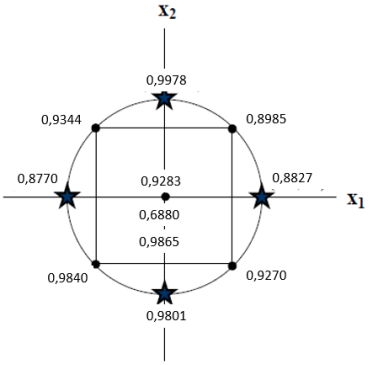

Figure 46. Experimental design and the measured values for sphericity for 25 degrees.

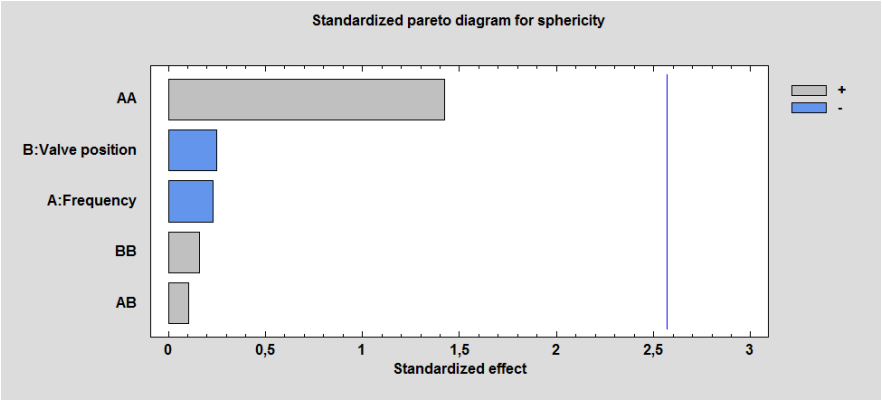

Figure 47. Standardized pareto diagram for sphericity for 25 degrees.

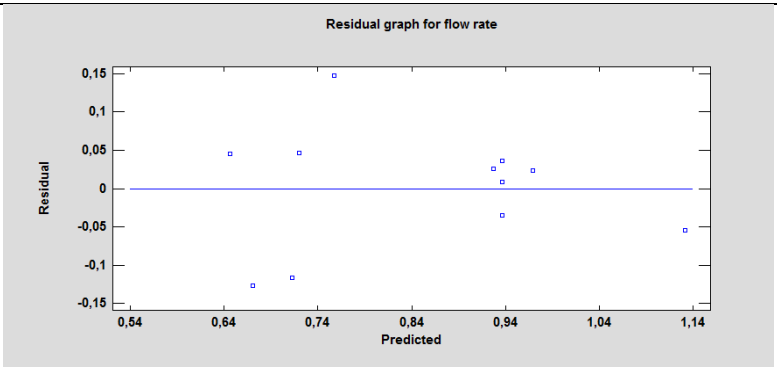

Figure 48. Residual graph for flow rate for 25 degrees.

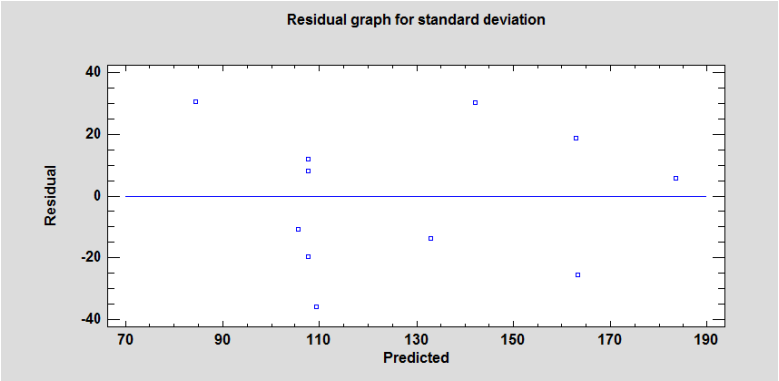

Figure 49. Residual graph for standard deviation for 25 degrees.

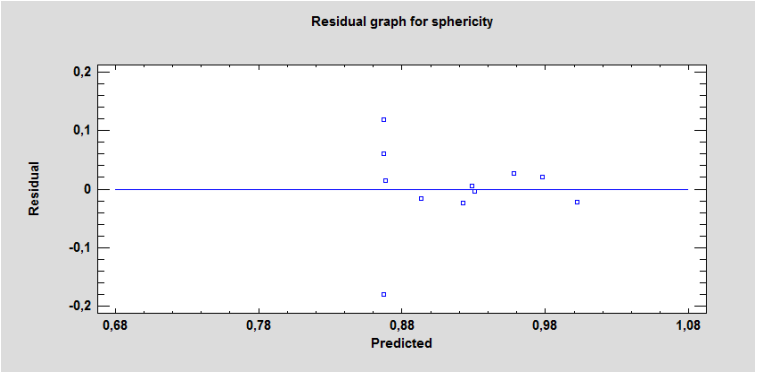

Figure 50. Residual graph for sphericity for 25 degrees.